Specificity of TRH receptor coupling to G-proteins for regulation of ERG K^+ channels in GH_3 rat anterior pituitary cells

Pablo Miranda, Teresa Giráldez, Pilar de la Peña, Diego G. Manso, Carlos Alonso-Ron, David Gómez-Varela, Pedro Domínguez and Francisco Barros

Departamento de Bioquímica y Biología Molecular, Edificio Santiago Gascón, Campus del Cristo, Universidad de Oviedo, E-33006, Oviedo, Asturias, Spain

The identity of the G-protein coupling thyrotropin-releasing hormone (TRH) receptors to rat *ether-à-go-go* related gene (r-ERG) K^+ channel modulation was studied *in situ* using perforated-patch clamped adenohypophysial GH_3 cells and dominant-negative variants (Gα-QL/DN) of G-protein α subunits. Expression of dominant-negative $G\alpha_{q/11}$ that minimizes the TRH-induced Ca^{2+} signal had no effect on r-ERG current inhibition elicited by the hormone. In contrast, the introduction of dominant-negative variants of $G\alpha_{13}$ and the small G-protein Rho caused a significant loss of the inhibitory effect of TRH on r-ERG. A strong reduction of this TRH effect was also obtained in cells expressing either dominant-negative $G\alpha_s$ or transducin α subunits, an agent known to sequester free G-protein $\beta\gamma$ dimers. As a further indication of specificity of the dominant-negative effects, only the dominant-negative variants of $G\alpha_{13}$ and Rho (but not $G\alpha_s$-QL/DN or $G\alpha_t$) were able to reduce the TRH-induced shifts of human ERG (HERG) activation voltage dependence in HEK293 cells permanently expressing HERG channels and TRH receptors. Our results demonstrate that whereas the TRH receptor uses a $G_{q/11}$ protein for transducing the Ca^{2+} signal during the initial response to TRH, this G-protein is not involved in the TRH-induced inhibition of endogenous r-ERG currents in pituitary cells. They also identify G_s (or a G_s-like protein) and G_{13} as important contributors to the hormonal effect in these cells and suggest that $\beta\gamma$ dimers released from these proteins may participate in modulation of ERG currents triggered by TRH.

(Received 28 February 2005; accepted after revision 12 May 2005; first published online 19 May 2005)
Corresponding author F. Barros: Departamento de Bioquímica y Biología Molecular, Edificio Santiago Gascón, Campus del Cristo, Universidad de Oviedo, E-33006, Oviedo, Asturias, Spain. Email: fbarros@correo.uniovi.es

Regulation of *ether-à-go-go* related gene (ERG) K^+ channel activity by the hypothalamic neuropeptide thyrotropin-releasing hormone (TRH) constitutes an essential point of hormonal control of electrical activity, and hence of intracellular Ca^{2+} levels ($[Ca^{2+}]_i$) and the secretory response in anterior pituitary cells (Barros *et al.* 1994, 1997; Weinsberg *et al.* 1997; Bauer, 1998; Bauer *et al.* 1998, 1999). The human ERG (HERG) channel has been also recognized as an important determinant of action potential characteristics in heart muscle and its inhibition by inherited mutations or a panoply of cardiac- and noncardiac-related prescribed drugs has been associated with an increased risk of cardiac arrhythmia and sudden death (Chiang & Roden, 2000; Keating & Sanguinetti, 2001; Redfern *et al.* 2003; Finlayson *et al.* 2004). Interestingly, the observation that arrhythmogenic syncopes are usually associated with physical, emotional or auditory stress suggests a link between hormonal (e.g. adrenergic) stimulation and cardiac ion channel function including HERG (Thomas *et al.* 2004). Furthermore, ERG channels also seem to play a key role setting the electrical behaviour of other cell types including neurones and glial, chromaffin, pancreatic β and tumour cells (Zhou *et al.* 1998*a*; Emmi *et al.* 2000; Rosati *et al.* 2000; Gullo *et al.* 2003; Sacco *et al.* 2003; Lastraioli *et al.* 2004). Nevertheless, unlike the relatively well known molecular and kinetic characteristics of ERG channels and in spite of their physiological and pathological relevance, many of their molecular mechanisms of regulation by different physiological agents remain unclear.

In native lactotrophs and clonal GH adenohypophysial cells, endogenous ERG currents are inhibited by activation of the G protein-coupled TRH receptor (TRH-R; Bauer *et al.* 1990, 1994; Barros *et al.* 1992, 1993; Schäfer *et al.*

 DOI: 10.1113/jphysiol.2005.085803

1999; Schledermann *et al.* 2001). The TRH-R is coupled to a G-protein of the $G_{q/11}$ family (reviewed in Gershengorn & Osman, 1996) resulting in phospholipase C (PLC) activation and generation of *myo*-inositol 1,4,5-trisphosphate (IP_3) and diacylglycerol (DAG) from phosphatidylinositol 4,5-bisphosphate (PIP_2). It is also known that TRH is able to activate several PKC isozymes in GH_3 cells (Kiley *et al.* 1991; Akita *et al.* 1994). However, TRH-induced inhibition of ERG current in these cells does not depend on PKC or PKA activation (Bauer *et al.* 1990, 1994; Barros *et al.* 1992, 1993; Schäfer *et al.* 1999; Schledermann *et al.* 2001). Whether $G_{q/11}$ protein transduction, typically linked in many cells (including adenohypophysial cells) to Ca^{2+} signalling, plays a role in ERG channel regulation remains controversial. Thus, a pathway for ERG regulation by TRH involving a G_{13}- and Rho-mediating signalling cascade has been described in whole-cell voltage-clamped GH_4C_1 cells (Storey *et al.* 2002), but the relative importance of this transduction pathway as compared with the 'classical' $G_{q/11}$-mediated TRH-induced signalling was not assessed. Furthermore, $G_{q/11}$ but not $G_{i/o}$ or G_{13} has been recently shown to mediate muscarinic inhibition of ERG currents in tsA-201 cells coexpressing rat ERG1 channels and M1 muscarinic receptors (Hirdes *et al.* 2004). In adenohypophysial cells, the $G_{q/11}$-mediated coupling of TRH-R to PIP_2 hydrolysis leads to an initial elevation of $[Ca^{2+}]_i$ via IP_3 that mediates a peak of secretion associated with a transient hyperpolarization of the cell membrane due to activation of Ca^{2+}-dependent K^+ channels (Gómez-Varela *et al.* 2003*b*). However, normal inhibition of ERG channel activity in response to TRH has been observed in individual cells in which the initial Ca^{2+} response is totally absent (Barros *et al.* 1991, 1992, 1994). Although the PKC branch of the PLC signalling cascade is necessary for reversal of the TRH-induced ERG inhibition in GH_3 cells (Gómez-Varela *et al.* 2003*b*) and PIP_2 depletion could lead to HERG current reduction in HEK293 cells (Bian *et al.* 2001), the TRH-induced inhibition of the GH_3 cell r-ERG current also takes place after blockade of PIP_2 consumption with a PLC inhibitor (Gómez-Varela *et al.* 2003*b*). These results and the reported modification of the TRH effects on r-ERG in cholera toxin-treated GH_3 cells (Barros *et al.* 1994; Bauer *et al.* 1994) open the possibility that, at least in adenohypophysial cells, a transduction cascade(s) involving either a G_s-like protein or a G_{13}- and Rho-based pathway, couples the TRH-R to endogenous ERG channel inhibition.

In this report we use double mutants (Gα-QL/DN) of G-protein α subunits able to act as dominant-negative inhibitors against specific G-proteins (Yu *et al.* 2000) to explore the specificity of TRH-R coupling to G-proteins for ERG K^+ channel inhibition in GH_3 rat anterior pituitary cells. Our results demonstrate that whereas the TRH-R certainly uses a $G_{q/11}$ protein for transducing the Ca^{2+} signal during the initial response to the hormone, this G-protein is not involved in the TRH-induced inhibition of ERG currents. Dominant-negative variants of $G\alpha_{13}$ and Rho, but not of $G\alpha_{q/11}$, are able to significantly reduce the inhibitory effect of TRH on ERG. Furthermore, a prominent reduction is observed upon introduction of dominant-negative $G\alpha_s$. Interestingly, a strong reduction of the TRH-induced inhibition is also observed in cells overexpressing transducin α subunits ($G\alpha_t$), an agent known to sequester free G-protein $\beta\gamma$ dimers (Crespo *et al.* 1994; Faure *et al.* 1994; Palomero *et al.* 1998). The specificity of the dominant-negative and $G\alpha_t$ effects is demonstrated by their failure to modify the Ca^{2+} response in the same cells. Furthermore, dominant-negative $G\alpha_{q/11}$ (but not $G\alpha_t$ or dominant-negative $G\alpha_s$, $G\alpha_{13}$ and Rho) was able to reduce TRH-induced release of Ca^{2+} from intracellular stores in HEK293 cells permanently expressing HERG channels and TRH-Rs. In these cells, however, only the dominant-negative forms of $G\alpha_{13}$ and Rho (but not $G\alpha_t$ or dominant-negative $G\alpha_s$) were able to antagonize the modifications in activation voltage dependence induced by TRH on HERG currents. On the other hand, only $G\alpha_t$ and dominant-negative $G\alpha_{q/11}$ expression reduced the TRH-induced HERG current inibition at positive voltages. Apart from emphasizing the specificity of the different dominant-negative constructs, this also suggests that the cellular background and/or the channel isoform may influence the transduction mechanism(s) involved in hormonal regulation of ERG.

Methods

Plasmids and chemicals

The original plasmid containing the cDNA for the HERG channel was a generous gift of Dr E. Wanke (University of Milan, Italy). pEGFP-N3 plasmid was obtained from Clontech. pcDNA3.1 plasmids containing dominant-negative forms of $G\alpha_q$ ($G\alpha_q$-Q209L/D277N), $G\alpha_{13}$ ($G\alpha_{13}$-Q266L/D294N), $G\alpha_s$ ($G\alpha_s$-Q227L/D295N) and RhoA (RhoA-T19N 3xHA-tagged-NH2) were obtained from Guthrie (Guthrie cDNA Resource Center; currently transferred to University Missouri-Rolla cDNA Resource Center, Rolla, MO, USA). $G\alpha_t$ was cloned in pcDNA3 as an *Eco*RI/*Xho*I fragment transferred from pcDNAI (provided by Dr J. S. Gutkind, N. I. of Dental Research, N.I.H., Bethesda, MD, USA). TRH and nystatin were purchased from Sigma. E-4031 and anti-HERG polyclonal antibodies were from Alomone Laboratories; Fura-2 and Fura-2/AM were from Molecular Probes.

GH_3 cell culture and transfection

GH_3 rat anterior pituitary cells (ATCC-CCL 82.1) were plated in 35-mm diameter tissue culture plastic dishes containing sterile glass coverslips coated with poly L-lysine

and grown at 37°C in a humidified atmosphere of 95% air and 5% CO_2. The culture medium consisted of a 1 : 1 mixture of Dulbecco's modified Eagle's medium and Ham's F-12 nutrient mixture (Sigma) supplemented with 100 U ml^{-1} penicillin, 1.1 mg ml^{-1} streptomycin and a serum mixture of 15% horse serum and 2.5% fetal bovine serum. The coverslips constituted the bottom of a small recording chamber (0.2–0.3 ml) that was continuously perfused with saline at a rate of about 1 ml min^{-1}. Cells trypsinized 24 h prior to transfection lying in poly-L-lysine-coated coverslips were transiently transfected using Lipofectamine 2000 according to the manufacturer's instructions (Invitrogen, Carlsbad, CA, USA). Unless otherwise indicated, 5.0 μg of plasmids containing the different constructs and pEGFP-N3 codifying green fluorescent protein (eGFP) as a marker for transfection in a 10 : 1 ratio were used. The mixture of 5.5 μg of total DNA and Lipofectamine was incubated in serum-free medium for 20 min and added to the plates containing the cells in serum-containing medium without antibiotics. Recordings were performed 24–48 h after transfection.

Generation and isolation of permanently transfected HEK 293 cell clones

HERG channel cDNA was subcloned into *Hin*dIII/*Bam*HI sites of the pcDNA3 vector (Invitrogen). Monolayer cultures (~50% confluent) of human embryonic kidney cells (HEK293; ATCC CRL-1573) were transfected with this construct using Lipofectamine (Gibco). Three days after transfection, the cells were trypsinized and diluted in a medium containing 1 mg ml^{-1} geneticin. Subsequently they were cultured until cell colonies were visible. Individual colonies were picked with cloning cylinders and tested for HERG currents. A clone named H36 was selected for further transfection. Cells of clone H36 were cotransfected with plasmid pcDNA3.1/Hygro(+) (Invitrogen) containing the cDNA for the TRH-R (de la Peña *et al.* 1992) inserted between the *Hin*dIII/*Xba*I sites of the vector. Hygromycin B (150 μg ml^{-1}) was used to select H36 clones coexpressing HERG channels and TRH-Rs. We chose for further work a clone named HEK-H36/T1 showing: (a) robust HERG currents under voltage-clamp, (b) reproducible calcium responses when perfused with TRH after loading the cells with the fluorescent Ca^{2+} indicator Fura-2, and (c) a predominant level of a 155 kDa band of HERG protein, corresponding to the mature and more glycosylated HERG likely to be located in the plasma membrane (Zhou *et al.* 1998*b*; Petrecca *et al.* 1999), immunodetected in cell extracts with HERG-specific antibodies. Cells were grown at 37°C in a humidified atmosphere of 95% air and 5% CO_2. HEK 293 cells were cultured in the same medium as GH_3 cells supplemented with 100 U ml^{-1} penicillin, 0.1 mg ml^{-1} streptomycin and 10% fetal bovine serum. HEK-H36/T1 cells were maintained in the presence of 1 mg ml^{-1} geneticin sulphate and 150 μg ml^{-1} hygromycin B (Gibco) and plated on the poly-L-lysine-coated coverslips for recording. Transient transfection of HEK-H36/T1 cells was performed following the procedures indicated above for the GH_3 cells.

Electrophysiological recordings, solutions and data analysis

Current recordings were performed at room temperature with the perforated-patch variant of the patch-clamp technique as previously described (Barros *et al.* 1991, 1992, 1994, 1997; Gómez-Varela *et al.* 2003*b*). Electrodes were fabricated from borosilicate or kimax disposable micropipettes (Boralex, Rochester Scientific, Rochester, NY; Fisherbrand, Fisher Scientific, Pittsburg, PA or Kimble glass Inc., Vineland, NJ, USA). Electrode resistance amounted 2–5 MΩ when filled with the pipette solution containing (mM): 65 KCl, 30 K_2SO_4, 10 NaCl, 1 $MgCl_2$, 50 sucrose and 10 Hepes (pH 7.4 with KOH). The tip of the pipette was initially filled with nystatin-free solution and the remainder of the pipette was back-filled with the same solution also containing 250 μg ml^{-1} nystatin, added from a stock of 50 mg ml^{-1} nystatin freshly dissolved in dimethylsulphoxide. These solutions were sonicated just before use. The course of perforation was followed by monitoring the progress of capacitive transients under voltage-clamp mode, setting the pipette voltage at a value of −70 mV. Access resistance, as estimated from the capacitive compensation circuitry on the amplifier, reached 10–30 MΩ within 5–20 min after the seal was made. Solution junction potentials were nulled before seal formation. Once patch permeabilization reached the indicated levels, the extracellular solution was changed as indicated and the cell was voltage-clamped at the desired holding potential. An EPC-7 patch-clamp amplifier (HEKA Elektronic, Lambrecht, Germany) was used to record membrane currents. Stimulation, data acquisition and analysis were carried out using Pulse and PulseFit software (HEKA Elektronic) running on Macintosh computers. Current records were sampled every 1 ms and digitally filtered at 500 Hz. r-ERG current data are shown without correction for leakage and capacitative transients. A P/n method was used for leak and capacitive current subtraction of the HERG recordings in HEK-H36/T1 cells. Further data processing was performed with PulseFit and Igor Pro (WaveMetrics, Lake Oswego, OR, USA).

The standard extracellular saline used for perforation and monitoring $[Ca^{2+}]_i$ contained (mM): 137 NaCl, 4 KCl, 1.8 $CaCl_2$, 1 $MgCl_2$, 10 glucose, and 10 Hepes (pH 7.4

with NaOH). Recordings of r-ERG currents in GH_3 cells were performed after changing the extracellular medium to high-K^+, Ca^{2+}-free solution once permeabilization of the patches had been completed. This solution contained (mM): 140 KCl, 4 $MgCl_2$, 10 EGTA and 10 Hepes titrated to pH 7.4 with KOH. Inward currents were studied during hyperpolarization pulses to −100 mV from a holding potential of −10 mV. The hyperpolarization pulses were preceded by a 100 ms ramp from 0 to −50 mV that can yield an estimation of the membrane conductance within this voltage range and would tend to potentiate the otherwise voltage-dependent effect of TRH (Bauer *et al.* 1990; Barros *et al.* 1992, 1994, 1997). To prevent variations due to differences in deactivation rates from cell to cell, the magnitude of the inward currents was estimated with the PulseFit software as the total inward charge computed between cursors located at 0.5 and 100% duration of the hyperpolarization pulses. HERG currents were recorded in HEK-H36/T1 cells in standard extracellular saline following the pulse protocols indicated on the figures. Kinetic parameters of activation and deactivation were obtained as previously described (Barros *et al.* 1998; Viloria *et al.* 2000). The voltage dependence of current activation was assessed using standard tail current analysis. Tail current magnitudes normalized to maximum were fitted with a Boltzmann function:

$$h(V) = I_{\max}[1/(1 + \exp((V - V_{1/2})/k))]$$

where V is the test potential, $V_{1/2}$ is the half-activation voltage, and k is the slope factor. Steady-state voltage dependencies of activation were obtained as previously described (Viloria *et al.* 2000) applying depolarization pulses of variable magnitude and up to 10 s duration from two holding potentials: +40 mV to hold the channels fully open and −80/−100 mV to hold them fully closed. The position of the Boltzmann curves under true steady-state conditions was estimated as an extrapolated mean from the curves obtained at both holding potentials to ensure that they were a function exclusively of depolarization pulse characteristics, regardless of the previous (open or closed) state of the channels. The time course of activation was monitored using an indirect envelope of tail current protocol (Viloria *et al.* 2000), varying the duration of the depolarization pulse and following the variation in the magnitude of the tail currents recorded after going back to a negative voltage. The rates of deactivation were determined from negative-amplitude biexponential fits to the decaying phase of tail currents. The first cursor of the fitting window was advanced to the end of the initial hook due to the recovery of inactivation.

Intracellular calcium measurements

Measurements of intracellular Ca^{2+} concentrations ($[Ca^{2+}]_i$) were performed in cells platted in poly-L-lysine-coated coverslips as indicated above. In this case the coverslips were transferred to wells containing standard extracellular saline plus 5 μM Fura-2/AM (Molecular Probes) and loaded with the dye for about 60 min at room temperature. After loading with Fura-2, cells were washed with saline to remove non-hydrolysed Fura-2/AM and left for another 30 min before recording to facilitate AM hydrolysis by cellular esterases. Fluorescence measurements were performed in a Axiovert 100 microscope equipped with a Plan-NeoFluar 40×/0.75 objective and epifluorescence accessories (Carl Zeiss), attached to a fluorescence imaging system (TILL-Photonics GmbH, Martinsried, Germany). Control of the monochromator (Polychrome IV) and the 12-bit cooled CCD camera (IMAGO) was performed using TILLvisION imaging software. Cells were excited through a dichroic mirror reflecting less than 395 nm light. Fluorescence signals were filtered through a 410 nm long-pass filter. Cycles of sample excitation were repeated every 500 ms consisting in 10/20 ms periods of irradiation with 340, 360 and 380 nm light. The ratio of the emission intensities (340 nm/380 nm) was used as a measure for changes in intracellular Ca^{2+}. When eGFP-transfected cells were used, a correction for eGFP fluorescence due to residual eGFP excitation at 340–380 nm was performed. Using eGFP-containing cells without Fura-2 we estimated previously that 13% of the fluorescence recovered above 510 nm (using a GFP filter set with a 500 nm dichroic and a 510 nm long-pass filter) following eGFP excitation at 488 nm is also present upon eGFP excitation at 380 nm using the conventional Fura-2 set-up. Less than 1% was recovered when eGFP was excited at 340 nm. Subsequently, the eGFP-derived fluorescence at 380 nm was estimated in every individual cell loaded with Fura-2 from the (13%) fluorescence intensity at 488 nm (a wavelength at which Fura-2 is not excited). This amount was subtracted from the total fluorescence at 380 nm to isolate the Fura-2-specific signal. Ca^{2+} concentrations were estimated from the 340 nm/380 nm fluorescence ratio by comparison with Fura-2 standards (Barros *et al.* 1994).

Statistics

Data values given in the text and in figures with error bars represent the mean ± S.E.M. for the number of indicated cells. Comparison between data groups was at first performed by parametric Student's unpaired t test (2-tailed) or ANOVA. Due to dispersion of the data in individual cells after some treatments (e.g. $G\alpha_{13}$-QL/DN and RhoA T/N transfections in Fig. 4), non-homogeneous variances (as evidenced after a Bartlett's test) were sometimes obtained. Therefore, alternate Welch's test assuming Gaussian populations with unequal S.D.s and a non-parametric Wilcoxon or Mann-Whitney test that

does not make any assumption about the scatter of the data were also used to evaluate significance of mean differences between cell populations. For *a posteriori* comparison of two specific samples a Bonferroni or a Dunn test for multiple comparisons was also used following one-way ANOVA or Kruskal-Wallis non-parametric ANOVA tests, respectively. In all cases, P-values < 0.05 were considered as indicative of statistical significance.

Results

Validation of the dominant-negative strategy using $G\alpha_q$-QL/DN and the TRH-induced Ca^{2+} response of the GH_3 cells

To examine the transduction pathway leading to ERG inhibition upon TRH stimulation, we expressed xanthine nucleotide binding mutants of different G-protein α subunits. These mutants carrying a double mutation (leucine and asparagine substituting for a glutamine and an aspartate, respectively) possess a lowered affinity by guanine nucleotides and an enhanced affinity by xanthine nucleotides that make them form stable and specific complexes with cognate receptors and compete with endogenous wild-type G-proteins (Yu *et al.* 2000). We first probed the effectivity of this approach using dominant-negative $G\alpha_q$ ($G\alpha_q$-Q209L/D277N) and exploring the initial (Phase 1) TRH-dependent response of the GH_3 cells. This phase corresponds to a transient release of stored Ca^{2+} into the cytosol due to production of IP_3 by PLC-catalysed PIP_2 hydrolysis, leading to an initial and transient hyperpolarization of the cell membrane by activation of Ca^{2+}-dependent K^+ channels (Gómez-Varela *et al.* 2003*b*). We reasoned that blockade of this transduction pathway with $G\alpha_q$-QL/DN should minimize all the cellular responses that characterize this phase such as (i) the transient membrane hyperpolarization, (ii) the transient increase in potassium currents that determine this hyperpolarization, and (iii) the transient $[Ca^{2+}]_i$ increase that activates the Ca^{2+}-dependent K^+ currents. As shown in Fig. 1*A* the transient hyperpolarization of the cell membrane induced by TRH in perforated-patch current-clamped GH_3 cells is nearly abolished in cells expressing $G\alpha_q$-QL/DN (see averaged voltage traces in the insets). Interestingly, as shown in the individual cell recordings illustrated in Fig. 1*A*, the increase in the rate of production of action potentials (Phase 2 of hormone action) that follows the initial hyperpolarization was maintained in the presence of the dominant-negative. As a second validation of the dominant-negative effect, we studied the appearance of membrane currents immediately after TRH addition in patch-perforated voltage-clamped GH_3 cells bathed in high-K^+ Ca^{2+}-free solution. Figure 1*B* shows that the current increases induced by TRH were absent in cells expressing $G\alpha_q$-QL/DN. Thus, these increases represent $G\alpha_q$-mediated PLC activation and activation of K^+ currents by Ca^{2+} released from intracellular stores via IP_3, because they were determined without extracellular Ca^{2+}. Furthermore, the effect of $G\alpha_q$-QL/DN was specific since the TRH-induced currents remained unaltered in cells expressing the dominant-negative α subunit of G_{13}, a G-protein predictably unrelated to the PLC–IP_3 Ca^{2+} signalling pathway.

For an additional demonstration of the effectiveness and specificity of the dominant-negative approach we studied the effect of the $G\alpha$-QL/DN proteins on hormone-induced $[Ca^{2+}]_i$ increases. For this purpose, the fluorescence of Fura-2 was monitored in the transfected cells as indicated in Methods. As an internal control, TRH-induced variations in fluorescence of the cells present in the same microscope field but not expressing the transfection marker (eGFP) were monitored. We determined first that transfection or expression of the eGFP biosensor itself does not modify the $[Ca^{2+}]_i$ increases induced by the hormone, using GH_3 cells transfected with eGFP and pcDNA3B plasmid lacking any G-protein codifying insert. Data from a representative experiment indicate that whereas addition of 1 μM TRH raised $[Ca^{2+}]_i$ from a basal averaged value of 105 ± 32 nM ($n = 35$) to an initial maximum of 236 ± 32 nM in the 35 cells of a microscope field lacking eGFP fluorescence, the $[Ca^{2+}]_i$ level was increased from 80 ± 31 to 240 ± 29 nM in the 13 cells from the same field showing a clear eGFP expression. On the other hand, in both cases most of the cells showed a significant increase in peak $[Ca^{2+}]_i$ regardless of the presence or the absence of eGFP expression.

The aforementioned results strongly differ from those obtained with cells transfected with eGFP and a plasmid coding for $G\alpha_q$-QL/DN (Fig. 2*A*). In this case, TRH raised the basal $[Ca^{2+}]_i$ level of 73 ± 9 nM to 141 ± 14 nM in the 26 cells showing no detectable eGFP expression. In contrast, only a peak value of 61 ± 5 nM $[Ca^{2+}]_i$ from a basal level of 49 ± 6 nM was obtained upon TRH addition in the 11 cells of the same field showing a clear eGFP fluorescence. It is also important to note that in this case only 3 of the 11 cells expressing eGFP showed any significant increase in $[Ca^{2+}]_i$ as compared with the 18 in which $[Ca^{2+}]_i$ was clearly increased from 26 cells not expressing the transfection marker. Furthermore, whereas only a modest $[Ca^{2+}]_i$ increase from 61 ± 6 to 94 ± 4 nM was observed in those three cells expressing eGFP, a prominent initial peak of Ca^{2+} that raised $[Ca^{2+}]_i$ from 73 ± 9 to 172 ± 7 nM was obtained in the 18 cells in which eGFP (and hence $G\alpha_q$-QL/DN) expression was not detectable. Analogous results were obtained in two additional experiments. This demonstrates that (i) a much lower percentage of cells expressing the dominant-negative variant of $G\alpha_q$ respond to TRH, and (ii) even in the few cells expressing $G\alpha_q$-QL/DN that show a detectable response

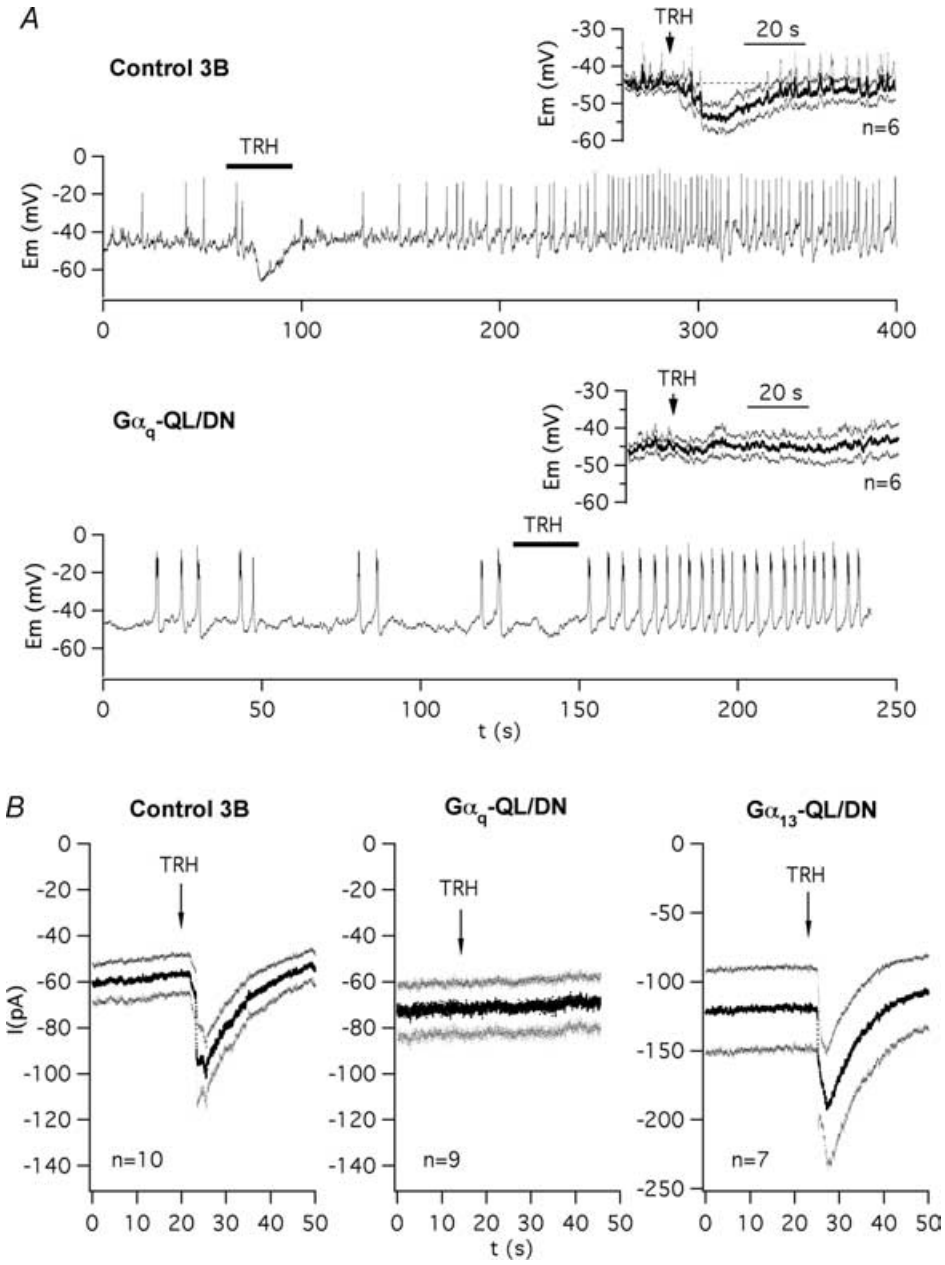

Figure 1. Blockade by dominant-negative $G\alpha_q$-QL/DN of the initial phase 1 of response induced by TRH in GH_3 cells

A, effect of dominant-negative $G\alpha_q$ on TRH-induced Phase 1 of hyperpolarization. Representative recordings of membrane potential are shown in two cells either expressing the dominant-negative form of $G\alpha_q$ (lower trace) or not (upper trace). Application of 1 μM TRH is marked with a horizontal line on top of the traces. Note the maintenance of Phase 2 of increased electrical activity in the $G\alpha_q$-QL/DN-transfected cell. Traces averaged point by point from several cells are shown in the insets. Continuous current traces averaged point by point and their corresponding S.E.M. are shown. In this cases, traces were synchronized to the time of TRH addition as indicated with an arrow. *B*, effect of dominant-negative $G\alpha_q$ and $G\alpha_{13}$ on Ca^{2+}-dependent K^+ currents elicited in GH_3 cells by TRH during the initial Phase 1 of response. Continuous current traces averaged point by point and their corresponding S.E.M. are shown for cells transfected with vector pcDNA3B (Control 3B), or with plasmids codifying the dominant-negative mutants of $G\alpha_q$ ($G\alpha_q$-QL/DN) and $G\alpha_{13}$ ($G\alpha_{13}$-QL/DN). Traces were synchronized to the time of 1 μM TRH addition as indicated with an arrow. High-K^+, low-Ca^{2+} extracellular solution and a potential of -30 mV were used for better detection of inward K^+ currents activated by Ca^{2+} released from intracellular stores via IP_3.

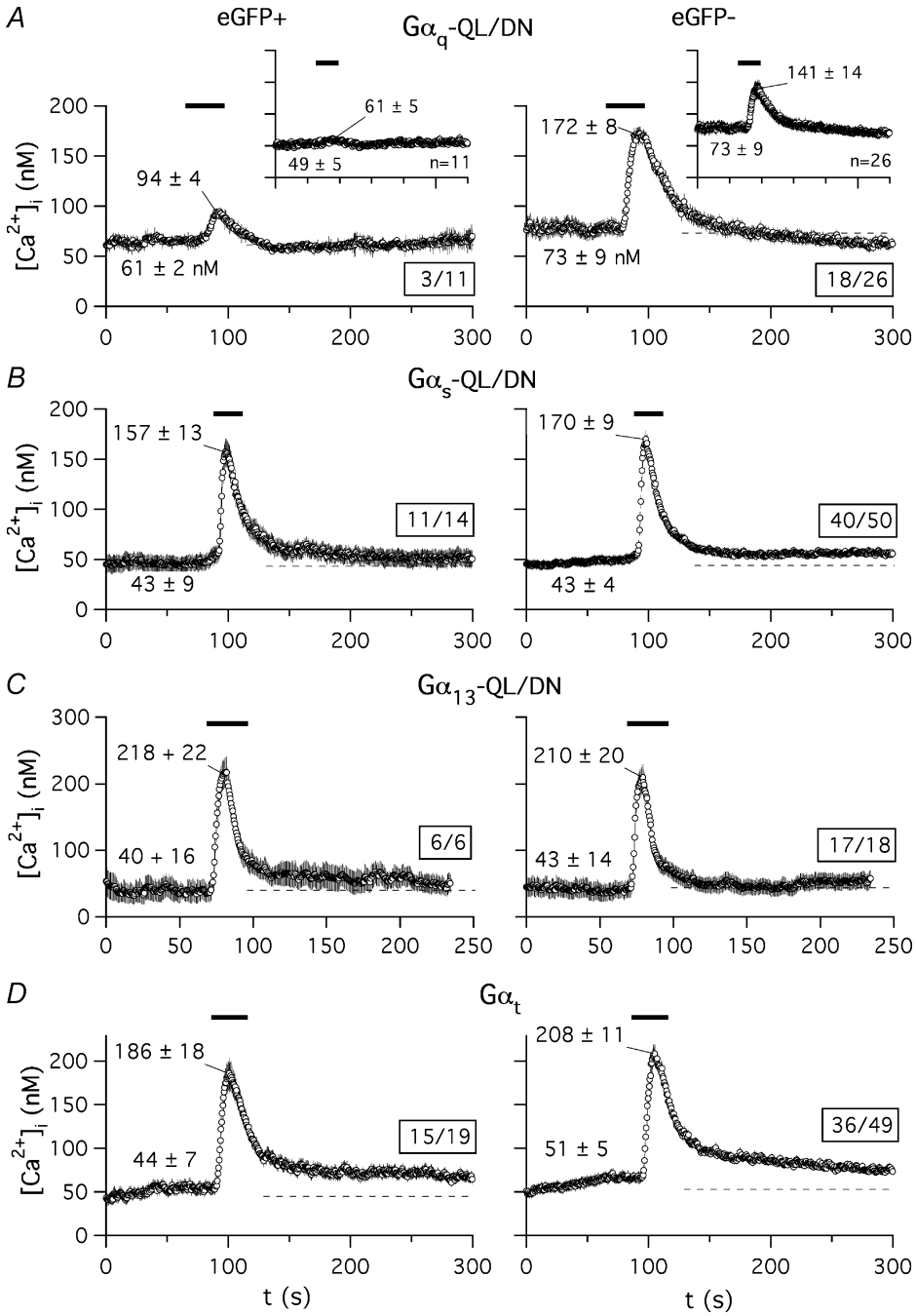

Figure 2. Effect of dominant-negative Gα subunits or $G\alpha_t$ expression on Ca^{2+} liberation from GH_3 cell intracellular stores in response to TRH

The time course of variations in $[Ca^{2+}]_i$ levels is shown for Fura-2 loaded cells from a microscope field transfected with $G\alpha_q$-QL/DN (*A*), $G\alpha_s$-QL/DN (*B*), $G\alpha_{13}$-QL/DN (*C*), or $G\alpha_t$ (*D*). Addition of 1 μM TRH is indicated by horizontal lines on top of the traces. Continuous traces averaged point by point and their corresponding S.E.M. are shown. Averaged basal levels are signalled by dashed lines. Data correspond to cells showing fluorescence of the transfection marker ($eGFP^+$, left) or not ($eGFP^-$, right). Variations of $[Ca^{2+}]_i$ levels in the cell subpopulations showing a detectable peak Ca^{2+} increase after visual inspection are illustrated. In all cases the number of averaged cells with respect to the total number of cells present in the field is boxed. Data from the whole cell population present in the microscope field are shown in the insets of panel *A*. Averaged values from all data points before TRH addition and that of the initial maximum are indicated. Analogous results were obtained in two additional experiments.

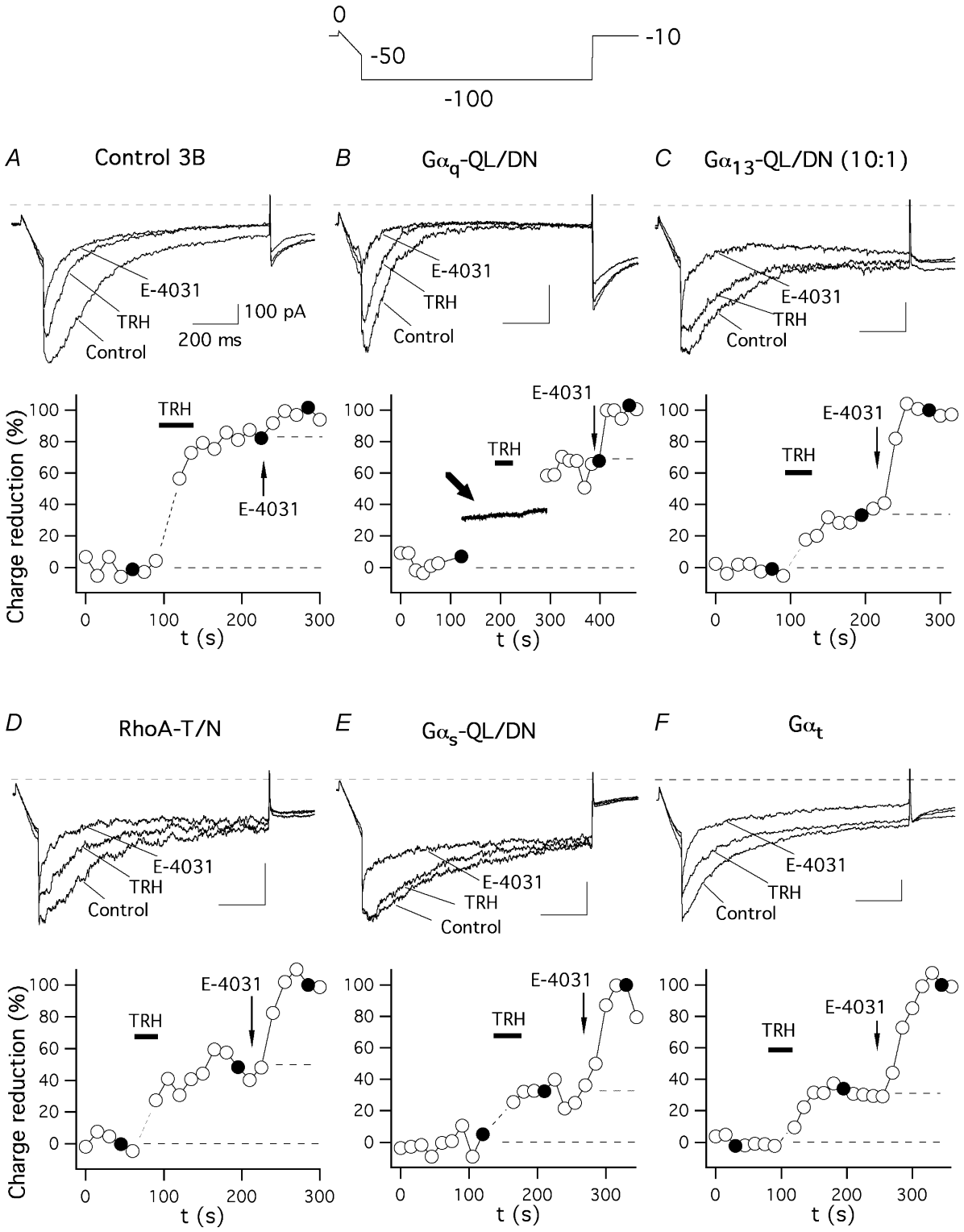

Figure 3. Effect of dominant-negative Gα subunits and $G\alpha_t$ on TRH-induced inhibition of endogenous r-ERG currents in GH_3 cells

The time course of relative r-ERG current reduction by TRH and E-4031 is shown for six different cells transfected with vector pcDNA3B (*A*), or with plasmids encoding the dominant-negative mutants of $G\alpha_q$ (*B*), $G\alpha_{13}$ (*C*), RhoA (*D*) and $G\alpha_s$ (*E*), or the α subunit of transducin (*F*). Currents were recorded during 1 s hyperpolarizing pulses to −100 mV from a holding potential of −10 mV. The hyperpolarization step was preceded by a 100 ms ramp from 0 to −50 mV (Gómez-Varela *et al.* 2003*b*). Current estimations were performed from total inward charge during the hyperpolarization steps at −100 mV as described in Methods. Averaged charge values before any addition

to the hormone, the magnitude of the $[Ca^{2+}]_i$ increase is clearly smaller than that of cells in which the transfection marker (and hence the dominant-negative $G\alpha_q$) has not been expressed.

Specificity of dominant-negative Gα subunits on TRH-induced Ca^{2+} response

The results presented above indicate that expression of the dominant-negative form of $G\alpha_q$ constitutes an efficient way to suppress the Gq-dependent initial Ca^{2+} response to TRH of the GH_3 cells. Whereas coupling of endogenous and heterologously expressed TRH-Rs to Gq for activation of PLC-mediated PIP_2 hydrolysis has been widely documented, it has been also reported that in GH cells the TRH-R can interact with a number of different G-proteins that may include G_{13}, G_i and G_s or a G_s-like protein (Storey *et al.* 2002; reviewed by Gershengorn & Osman, 1996). To check the possible specificity of the dominant-negatives we also studied the Ca^{2+} response in cells expressing the QL/DN variants of $G\alpha_s$ and $G\alpha_{13}$. The elevations of $[Ca^{2+}]_i$ in response to TRH remained the same in cells expressing either $G\alpha_s$-QL/DN (Fig. 2*B*) or $G\alpha_{13}$-QL/DN (Fig. 2*C*) as compared with cells from the same microscope field lacking eGFP expression. Similar results were obtained in cells expressing transducin α subunits (Fig. 2*D*; see also below). Furthermore, as in control cells transfected with pcDNA3B (see above) or in untransfected cells (not shown), most of the cells expressing dominant-negatives of $G\alpha_s$ or $G\alpha_{13}$ showed significant increases in peak $[Ca^{2+}]_i$. This indicates that whereas coupling of TRH-R to $G_{q/11}$ is indispensable for the TRH-evoked Ca^{2+} response, coupling to a G-protein of the G_s or G_{13} type is not required for this effect.

Effect of different dominant-negative Gα subunits on TRH-induced inhibition of endogenous r-ERG currents in GH_3 cells

To investigate the transduction cascade linking the TRH-R to r-ERG channel inhibition we always used perforated-patch conditions to minimize cell dialysis and to preserve intact the intracellular components necessary for the hormonal response. To isolate the r-ERG current present in GH_3 cells and to quantify its inhibition by TRH, high-K^+ low-Ca^{2+} extracellular solutions and established voltage protocols were used. Thus, due to the fast inactivation of ERG channels at depolarized potentials and the presence of several outwardly rectifying voltage- and calcium-dependent K^+ currents in GH_3 cells, currents were studied during hyperpolarization pulses to −100 mV from a holding potential of −10 mV (see Methods). High-K^+ low-Ca^{2+} extracellular solutions were also used to increase the amplitude of the inwardly rectifying r-ERG currents and to reduce Ca^{2+} currents and activation of Ca^{2+}-dependent K^+ currents (Bauer *et al.* 1990, 1999; Barros *et al.* 1992, 1997; Weinsberg *et al.* 1997). Furthermore, since under these conditions the TRH-induced current inhibition is almost exclusively exerted on ERG currents, 5 μM of the ERG-specific blocker E-4031 (a concentration that totally blocks the r-ERG current) was added at the end of the experiments to subtract the E-4031-insensitive currents from the initial ones and compare the difference between the TRH- and E-4031-blocked currents in every individual cell (see Gómez-Varela *et al.* 2003*b*). Representative examples of TRH effects on r-ERG currents in cells transfected with different G-protein α subunit variants are shown in Fig. 3. Only successfully expressing cells identified by their eGFP fluorescence were used for recording. As shown in Figs 3*A* and 4, the inhibitory effect of TRH on the E-4031-sensitive current was not modified by the transfection procedure. Thus, a value of 76.8 ± 2.7% ($n = 20$) was obtained in cells transfected with eGFP and pcDNA3B plasmid lacking any G-protein coding insert, as compared with the 78.6 ± 5.4% ($n = 8$) inhibition obtained in cells showing no detectable eGFP expression. Similar inhibitions have been previously reported under identical conditions using untransfected cells (Gómez-Varela *et al.* 2003*b*). Most importantly, the TRH-induced inhibition was the same in cells expressing dominant-negative $G\alpha_q$-QL/DN (74.8 ± 6.3%, $n = 6$). It is important to note that failure to significantly modify the TRH-induced inhibition of r-ERG was not due to lack of efficient expression of $G\alpha_q$-QL/DN, since the early increases in Ca^{2+}-dependent K^+ currents induced by TRH (a Gq-dependent and PLC/IP_3/Ca^{2+}-related effect, see above) were absent in the same cells (Fig. 3*B*). Apart from adding further support to specificity of the $G\alpha_q$-QL/DN for the Ca^{2+} response, this indicates that whereas the

and those corresponding to the minimum following addition of 5 μM E-4031 were considered as 0 and 100%, respectively. Filled circles correspond to the current traces shown above. The first one or two data points following addition of TRH, when total inward currents become transiently enhanced by activation of Ca^{2+}-dependent K^+ channels due to massive liberation of Ca^{2+} from intracellular stores, have been deleted for clarity. Perfusion of 1 μM TRH and addition of E-4031 to the recording chamber are indicated. Values for the data in the absence and presence of TRH are indicated by horizontal dashed lines in the time courses. A continuous membrane current recording at a holding potential of −30 mV around the time of hormone addition is shown in *B* and marked with a thick arrow. Note the total absence of transient Ca^{2+}-dependent K^+ currents following TRH addition in the same cell showing a clear reduction of r-ERG currents. Similar results were obtained in the five additional cells expressing $G\alpha_q$-QL/DN.

TRH receptor certainly uses a $G_{q/11}$ protein for transduction of the Ca^{2+} signal during the initial response to the hormone, this G-protein is not involved in the TRH-induced inhibition of endogenous r-ERG currents in GH_3 cells.

Recent experiments in GH_4C_1 cells using a constitutively active mutant of $G\alpha_{13}$ and whole-cell recording showed a partial inhibition of r-ERG currents equivalent to that induced by TRH under similar conditions (Storey *et al.* 2002). Using our perforated-patch conditions, the inhibition of r-ERG by TRH was attenuated when the G_{13} pathway was antagonized with dominant-negative $G\alpha_{13}$. Thus, an inhibition of $56.4 \pm 6.9\%$ ($n = 12$, $P < 0.01$ *versus* control pcDNA3B-transfected cells, Welch and Mann-Whitney tests) in the E-4031-sensitive r-ERG currents was induced by TRH in cells transfected with 1.6 μg of plasmid encoding $G\alpha_{13}$-QL/DN (4 : 1 ratio *versus* EGFP plasmid; not shown). This value was slightly decreased to 43.8 ± 6.4 ($n = 15$) when 5.0 μg of the same plasmid were used (Figs 3*C* and 4). This effect was specific, as demonstrated by the total absence of $G\alpha_{13}$-QL/DN influence on TRH-induced Ca^{2+} responses (see above). Interestingly, the magnitude of the TRH-induced inhibition in individual cells showed a huge dispersion at both DNA concentrations, which made it appear that the 27 cell sample was composed of two subpopulations. Whereas nearly half of the cells showed TRH-induced r-ERG inhibitions above 50% (equivalent to those of controls and untransfected cells), a clear reduction of the hormonal effects leaving the TRH-induced inhibition below 50% took place in the other half of the cell population (see Fig. 4).

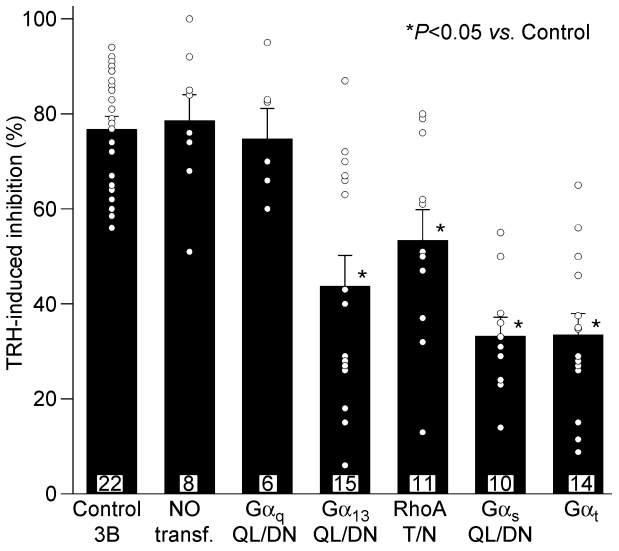

Figure 4. Percentage inhibition of r-ERG currents induced by TRH in GH_3 cells expressing dominant-negative $G\alpha$ subunits and $G\alpha_t$

Current inhibitions were estimated from total inward charge as described in Fig. 3. Data from individual cells averaged on the bars are shown as open circles. Values from cells transfected with dominant negative variants of $G\alpha_q$, $G\alpha_{13}$, RhoA and $G\alpha_s$, or transducin α subunits ($G\alpha_t$) are shown. Data from cells transfected with vector pcDNA3B (Control 3B) and from untransfected cells (NO transf.) are also shown for comparison. Significant variations among population medians as evidenced by Mann-Whitney test or ANOVA and *post hoc* multiple comparison test are indicated.

It has been shown that the activation of G_{13}- (and G_q-) dependent pathways is able to signal to different effectors through the small G-protein RhoA (Seasholtz *et al.* 1999; Sah *et al.* 2000; Dutt *et al.* 2002; Vogt *et al.* 2003). Expression of the dominant-negative RhoA-T19N also significantly attenuated r-ERG modulation by TRH, leaving a mean inhibition of $53.4 \pm 6.3\%$ ($n = 11$, $P < 0.01$ *versus* control, Welch and Mann-Whitney tests; Figs 3*D* and 4). Again, a considerable dispersion of the data was obtained in this case. Nevertheless, these data confirm previous results in GH_4C_1 cells and suggest that a transduction cascade involving G_{13} (but not G_q) and Rho may participate in the inhibition of ERG channels by TRH.

Previous results in GH_3 cells showed a modification of the TRH-induced effects on r-ERG in cells treated with the G_s-modifying agent cholera toxin (Barros *et al.* 1994; Bauer *et al.* 1994). Although a coupling of TRH-R to G_s with subsequent activation of adenylyl cyclase has been reported in GH_3 cells, evidence against (i) stimulation of the enzyme by TRH and (ii) specific down-regulation of $G\alpha_s$ following long-term expositions of GH_3 cells to TRH has been obtained also (reviewed in Gershengorn & Osman, 1996). Furthermore, a cholera toxin-dependent degradation of $G\alpha_s$ has been demonstrated in GH_3 cells (Chang & Bourne, 1989), but it is also known that cholera toxin treatment can cause a significant reduction in the number of TRH-Rs (Yajima *et al.* 1988). This prompted us to check whether antagonization of the Gs pathway with dominant-negative $G\alpha_s$ could cause any effect on the TRH-induced r-ERG current reductions. As shown in Figs 3*E* and 4, a prominent reduction of the inhibitory effect of TRH on r-ERG was observed in the presence of dominant-negative $G\alpha_s$-QL/DN. In this case, mean inhibition amounted only to $33 \pm 3.9\%$ ($n = 10$, $P < 0.0001$ *versus* control, Student's *t* and Mann-Whitney tests). This value is also significantly smaller than that obtained in the presence of RhoA-T19N ($P < 0.02$, Mann-Whitney test). It is important to note that in the presence of dominant-negative $G\alpha_s$ not only is the reduction of the TRH-induced inhibition the biggest observed, but also the dispersion of the data is notably reduced (Fig. 4). This supports the conclusion that G_s plays a crucial role on the inhibitory effects of TRH in GH_3 cells.

Effect of transducin α subunit expression on the TRH-induced inhibition of r-ERG in GH_3 cells

It has been recognized that receptors that activate G_{13} also couple to G_q and G_{11}. It is also well known that $G\alpha_{13}$ and $G\alpha_{q/11}$ signals induce Rho activation and subsequent

cellular responses by inducing GDP–GTP exchange in Rho guanine nucleotide exchange factors in response to extracellular stimuli (Seasholtz *et al.* 1999; Sah *et al.* 2000; Dutt *et al.* 2002; Vogt *et al.* 2003). Thus it seemed surprising that dominant-negative G_s (but not G_q), G_{13} and Rho share antagonism on the TRH-induced effects on r-ERG. To check the possibility that reduction of TRH-induced inhibition involves a component common to G_s and G_{13} but not available in heterotrimeric G_q, we studied the consequences of expressing transducin α subunits ($G\alpha_t$), a scavenger of $\beta\gamma$ dimers after they are released from G-proteins by receptor stimulation (Crespo *et al.* 1994; Faure *et al.* 1994; Palomero *et al.* 1998). The inhibition of r-ERG by TRH was strongly attenuated by $G\alpha_t$ ($33.5 \pm 4.4\%$; $n = 14$, $P < 0.0001$ *versus* control, Student's t and Mann-Whitney tests; Figs 3*F* and 4) up to levels equivalent to those observed with dominant-negative $G\alpha_s$. This effect of $G\alpha_t$ was totally specific, since both the percentage of cells showing a detectable increase in peak $[Ca^{2+}]_i$ and the magnitude of the TRH-induced Ca^{2+} response remained the same regardless of the presence or the absence of $G\alpha_t$ (Fig. 2*D*). As discussed below, this suggests that free $\beta\gamma$ subunits released from G_s (and perhaps shared by G_{13}) heterotrimers may be responsible for the TRH-induced inhibition of endogenous r-ERG currents in GH_3 cells.

Generation of a HEK293 cell clone permanently expressing HERG channels and TRH receptors and characterization of the TRH response

Unlike the strong and quite reproducible current inhibitions induced by TRH on the endogenous ERG current, only modest effects of the hormone have been reported on other kinetic characteristics of ERG either endogenous or heterologously expressed in GH_3 cells (Barros *et al.* 1992; Bauer *et al.* 1998; Schledermann *et al.* 2001). This fact and the sometimes variable effect of dominant negatives in the individual cells prevented us from reaching any consistent conclusion about the way in which different G proteins could be affecting other current parameters in these cells.

HEK293 cells permanently expressing HERG constitute an interesting and widely used model system to study easily the biochemical and electrophysiological properties of the channel (Zhou *et al.* 1998*b*). For this reason, we initially isolated several cell clones expressing HERG. Subsequently, they were cotransfected with a plasmid containing the TRH-R cDNA (de la Peña *et al.* 1992). Single colonies were selected and tested for both HERG current under voltage-clamp and TRH-induced Ca^{2+} responses with the fluorescent Ca^{2+} indicator Fura-2 (see Methods). A cell line named HEK-H36/T1 showing high HERG current density and also systematic Ca^{2+} increases when exposed to TRH was used for the experiments reported here. As shown in Fig. 7, the HEK-H36/T1 cells showed voltage-activated K^+ currents typical of HERG under the perforated-patch conditions chosen to maintain as intact as possible the hormonal responses. Apart from HERG currents, we frequently detected also other outward K^+ currents during the depolarization steps. The magnitude and the degree of inactivation of these currents during the depolarization pulses were highly variable. Nevertheless, their contribution was negligible along the tail current time course, as evidenced by their absence after treating the cells with the specific HERG inhibitor E-4031 (Fig. 5*A*). Thus only HERG current characteristics would be referred to by limiting the analysis to tail currents. Addition of TRH to HEK-H36/T1 cells loaded with Fura-2 triggered a transient increase in cytoplasmic Ca^{2+} that slowly declined to basal values upon hormone washout. On the average, the amplitude of this Ca^{2+} response was equivalent to that elicited in the same cells by carbachol (data not shown) probably acting through the endogenous muscarinic receptors of HEK293 cells. The TRH-induced Ca^{2+} responses were absent in the cell clones containing HERG channels but not coexpressing TRH-Rs.

The simultaneous presence of TRH-R and HERG channels in HEK-H36/T1 cells prompted us to check the effect of the hormone on HERG currents in this putatively simple and defined cellular background. TRH reduced tail HERG currents within 1–3 min after introducing the hormone in the recording chamber (Fig. 5*A*). The current level was lowered by $36 \pm 2\%$ ($n = 38$) when measured at the peak of the tails that followed pulses of 1 s duration at +40 mV. Furthermore, a strong shift in current availability voltage dependence to more positive voltages was also caused by TRH. Thus the $V_{1/2}$ value of the Boltzmann functions describing the I–V curves was shifted from -1.5 ± 1 to $+25.5 \pm 2$ mV ($n = 14$) under these conditions (Fig. 5*A*). It is important to note that the diminished tail currents remaining after treatment with TRH were entirely due to the operation of HERG channels, since they were abolished by E-4031.

Due to the slow activation and deactivation kinetics of HERG channels, no steady-state conditions would be expected within 1 s depolarizations. A possible cause of the shift in activation voltage dependence could be a displacement of the $V_{1/2}$ values to more depolarized potentials due to a slower activation rate leading to a less steady-state condition (Schönherr *et al.* 1999; Viloria *et al.* 2000). In fact, it is known that the activation rate of HERG channels in *Xenopus* oocytes is slowed by activation of coexpressed TRH-Rs (Barros *et al.* 1998). For this reason, we also tested the effects of TRH on HERG activation rates in HEK-H36/T1 cells using an indirect envelope of tail currents protocol (Barros *et al.* 1998; Viloria *et al.* 2000). As shown in Fig. 5*B*, the time required to attain a half-maximum current magnitude was increased by TRH near an order of magnitude between +40 and +60 mV.

Thus the difference in the inflection potentials of the *I–V* curves could be due, at least in part, to the different activation rates around the $V_{1/2}$ values. Nevertheless, an 18 mV shift from -22.5 ± 2.2 to -4.1 ± 2.8 mV ($n = 6$) was also detected in response to TRH when the *I–V* curves were generated from tail currents following long depolarization steps of 10 s duration (Fig. 6*A*). Finally, the position of the curves under real steady-state was

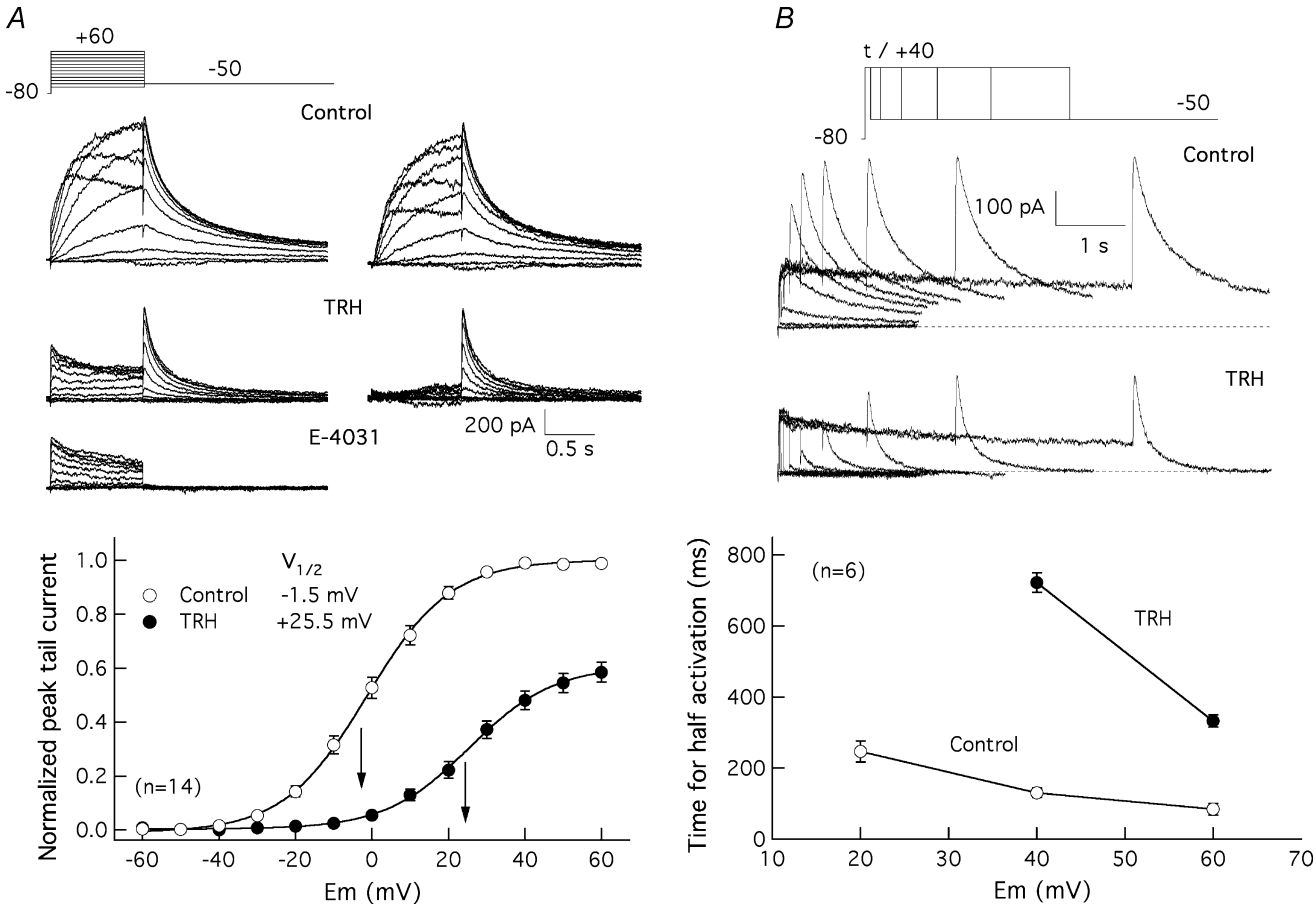

Figure 5. Effect of TRH on HERG current activation in HEK-H36/T1 cells
A, effect of TRH on voltage dependence of HERG current availability. The voltage dependence of activation was studied in the absence (Control) or the presence of 100 nM TRH (TRH) by varying the amplitude of a 1 s prepulse from a holding potential of −80 mV, and measuring the magnitude of the peak tail current at a constant repolarizing voltage of −50 mV. Membrane currents recorded in the presence of TRH plus 1 μM E-4031 (E-4031) are also shown for comparison. Superimposed current traces for depolarizing steps between −50 and +40 mV (Control) or −40 and +60 mV (TRH and E-4031) are shown on the left. Control and TRH traces obtained after subtracting the E-4031-resistant currents are also shown on the right. Pulses were applied once every 20 s. Current traces have been subtracted for leak. Recording of currents in the presence of TRH started 2 min after introducing the neuropeptide in the recording chamber. Averaged fractional activation curves obtained before and after addition of TRH are shown at the bottom. Normalized outward tail current magnitudes at the peak are plotted *versus* test pulse potential (E_m). Data normalized to maximum of tail current magnitude without TRH are presented. The continuous lines correspond to Boltzmann curves $h(V) = I_{max}(1/(1 + \exp(V - V_{1/2})/k))$, that best fitted the data. The relative position of the $V_{1/2}$ values and their numeric magnitude are indicated in the graph. *B*, effect of TRH on HERG current activation rate. The time course of voltage-dependent activation was studied by varying the duration of a depolarizing prepulse and measuring the magnitude of the peak tail current at a constant repolarizing voltage of −50 mV. Families of currents at a depolarizing potential of +40 mV are shown for a cell before (Control) and after adding 100 nM TRH (TRH). Current traces corresponding to depolarization steps of 0, 20, 40, 80, 160, 320, 640, 1280, 2560 and 5120 ms are shown superimposed. The dependence of activation rates on depolarization membrane potential is shown at the bottom. The magnitude of the peak tail current upon repolarization was determined from recordings as shown at the top. The time necessary to attain half-maximum current magnitude at different depolarization potentials is plotted in the absence or the presence of TRH.

extrapolated as the mean of those obtained from hyperpolarized (−80 mV) and depolarized (+40 mV) holding potentials (Schönherr *et al.* 1999; Viloria *et al.* 2000). In this case a 15 mV shift in $V_{1/2}$ (from −25.0 to −10.0 mV, $n = 2$) was obtained (Fig. 6*B*). Altogether, this suggests that two distinct effects on activation contribute to the shifts when studied with 1 s short depolarization steps: a genuine shift of the voltage dependence of activation and a marked slowing of activation rates moving the channels further away from steady-state conditions.

The deactivation properties of HERG can be obtained from the time course of current decay during voltage steps to negative potentials, following depolarizing pulses at a fixed time and voltage designed to activate (and inactivate) the channels. In this case, the closing time constants can be estimated by fitting a bi-exponential function to the decaying tail current phase that follows the initial peak once channel inactivation has been removed by the repolarization. Both the fast and the slow exponential components of current deactivation were significantly

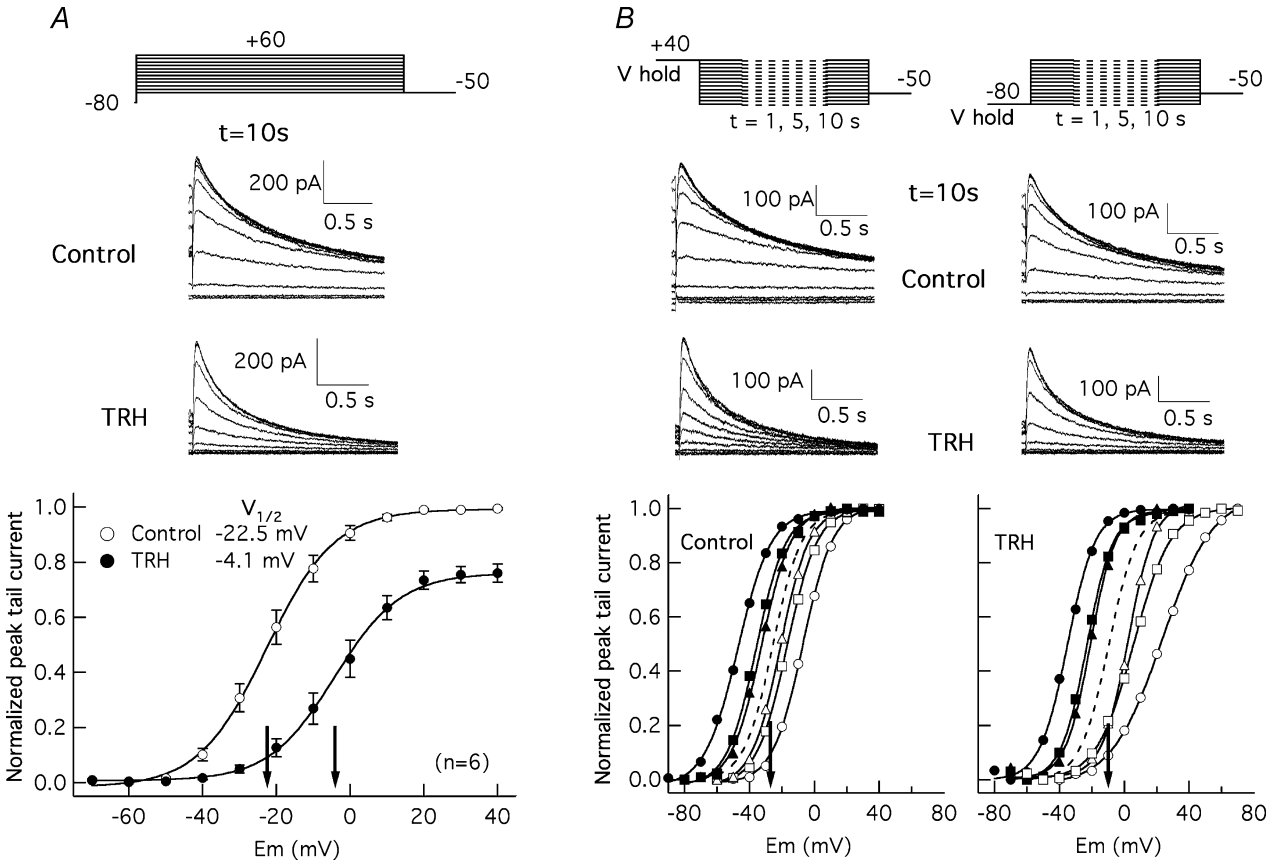

Figure 6. Effect of TRH on HERG activation voltage dependence under steady-state conditions
A, effect of TRH on activation voltage dependence studied using long depolarization steps of 10 s. Tail currents upon repolarization to −50 mV were obtained following 10 s depolarizations to different voltages as indicated at the top. Only the end of the depolarizing steps and the tail currents at −50 mV are shown for clarity. Traces correspond to a cell before (Control) and 3 min after introduction of 100 nM TRH (TRH). Averaged *I–V* curves before and after the hormonal treatments are shown at the bottom. The magnitude of the peak tail current upon repolarization was determined from recordings as shown at the top and normalized to maximum of tail current magnitude without TRH. *B*, effect of TRH on HERG steady-state voltage dependence of activation. Steady-state voltage dependence of activation was studied following the protocols shown in the two upper panels, with a prepulse of varying magnitude and a duration ranging from 1 to 10 s, followed by a pulse test to −50 mV. Holding potentials of +40 mV to keep the channels fully open and −80 mV to hold them fully closed were used as indicated. Families of currents during the test pulse for Control and TRH-treated cells following 10 s prepulses to different potentials are shown. Fractional activation curves before and after TRH treatment are shown at the bottom. Open and filled symbols correspond to data obtained from −80 and +40 mV holding voltages, respectively. Data obtained at prepulse duration of 1 s (circles), 5 s (squares), and 10 s (triangles) are plotted. In every curve current values were normalized to tail current magnitude in response to the more depolarized potential of the prepulse series. The dashed lines represent the deduced position of the activation curves under steady-state conditions obtained as a mean of those corresponding to both holding voltages and prepulses of 10 s duration. The $V_{1/2}$ values for the steady-state curves are indicated by arrows in the graphs.

accelerated by TRH at all voltages between −40 and −120 mV. As an example, the values of deactivation time constants at −50 mV for the fast and the slow components of closing were reduced by the hormone from 213 ± 22 to 119 ± 11 ms ($n = 5$, $P < 0.01$) and from 965 ± 135 to 579 ± 77 ms ($P < 0.05$, Student's t test), respectively.

The clear effects of TRH on HERG opening and closing contrast with the almost complete absence of hormone-induced modifications on inactivation properties. Thus only a slight but non-significant acceleration of inactivation rates was observed upon addition of TRH. Furthermore, both control and TRH-treated cells showed identical rates of inactivation recovery when the time course of the initial current increase in response to hyperpolarizing pulses was compared (not shown).

Effect of dominant-negative Gα subunits and Gα$_t$ on TRH-induced Ca^{2+} responses and modifications of HERG *I–V* curves in HEK-H36/T1 cells

The influence of the dominant-negatives and Gα$_t$ expression on the hormonal effects in HEK-H36/T1 cells was studied following procedures analogous to those described for endogenous channels in adenohypophysial GH_3 cells. Again, dominant-negative Gα$_q$, but not Gα$_t$ or dominant-negative Gα$_s$, Gα$_{13}$ and RhoA, reduced TRH-induced increases of cytoplasmic Ca^{2+} in the HEK-H36/T1 cells (Fig. 7). The modulation of HERG channels by TRH in HEK-H36/T1 cells was not changed by the transfection procedure used for dominant-negative expression (Control in Fig. 8). Surprisingly, the TRH-induced HERG current inhibition at positive voltages was not significantly altered in the presence of dominant-negative Gα$_{13}$, RhoA or Gα$_s$, but was strongly reduced by Gα$_q$-QL/DN or Gα$_t$ expression (Fig. 8*A* and *C*). On the other hand, the positive shifts in activation voltage dependence were reduced by RhoA-TN and nearly abolished by Gα$_{13}$-QL/DN (Fig. 8*A* and *B*). Although the shift in the *I–V* curves was almost absent in Gα$_q$-QL/DN-transfected cells, the basal position of the curves before adding hormone was clearly displaced to positive voltages in the cells expressing the dominant-negative form of Gα$_q$ (Fig. 8*A*). This complicates the interpretation of the dominant-negative Gα$_q$ influence on the hormonal effect in the *I–V* relation. Finally, expression of the βγ dimer scavenger Gα$_t$ left unaltered the TRH-induced voltage dependence shift in 10 of 14 tested cells, but blocked completely the reductions in maximal tail current magnitude triggered by the hormone. These results not only indicate a variation of the dominant-negative effects in different cellular and/or channel background, but also that these effects are differently manifested as a function of the channel parameter being considered.

Discussion

In this report we used a dominant-negative strategy to explore the specificity of TRH-R coupling to G-proteins for inhibition of the native r-ERG K^+ channels present in GH_3 rat anterior pituitary cells. Based in the reported insensibility of the TRH responses to pertussis toxin treatment (Bauer *et al.* 1994) we focused our efforts in the G_q, G_{13} and G_s families of G-proteins. Using the same approach we also compared the results with those obtained in an heterologous expression system, namely a HEK293 cell line (HEK-H36/T1) permanently expressing HERG channels and TRH-Rs. In both cases, xanthine nucleotide-binding (GαX) double mutants (Gα-QL/DN) of G-protein α subunits able to act as dominant-negative inhibitors against specific G-proteins (Yu *et al.* 2000) were used. Our results demonstrate that transduction of the Ca^{2+} signal during the GH_3 cell initial response to TRH is potently antagonized by dominant-negative Gα$_{q/11}$ and that this Ca^{2+} response remains unaltered in the presence of the dominant-negative variants of Gα$_{13}$, RhoA and Gα$_s$. On the other hand, dominant-negative variants of Gα$_{13}$ and Rho, but not of Gα$_{q/11}$, are able to significantly reduce the inhibitory effect of TRH on ERG. A more prominent reduction of the TRH-induced ERG inhibition is observed upon introduction of dominant-negative Gα$_s$. These results indicate that the TRH receptor certainly couples to a $G_{q/11}$ protein for transduction of the Ca^{2+} signal, but that this G-protein is not involved in the TRH-induced inhibition of ERG currents. This is coherent with previous results indicating that appearance of Phase 2 of increased electrical activity in GH_3 cells takes place in the presence or the absence of a detectable initial Ca^{2+} response (Phase 1; see Barros *et al.* 1994; Bauer *et al.* 1994). Our data also indicate that (i) failure to detect any influence of the Gα$_{13}$, Rho and Gα$_s$ dominant-negatives on the Ca^{2+} signal is not due to lack of their functional expression, (ii) coupling of the TRH-R to one (or more) heterotrimeric G protein(s) carrying Gα$_s$ and/or Gα$_{13}$ subunits takes place in the GH_3 cells, (iii) Gα$_s$ and perhaps a Gα$_{13}$- and Rho-dependent pathway can participate in the transduction cascade linking TRH-R activation to r-ERG modulation in GH_3 cells, and (iv) there is a clear specificity in the ability of dominant-negatives to antagonize different physiological responses triggered by TRH in these cells.

In principle, the observed specificity of the dominant-negatives seems rather surprising according to the proposed mechanism for negative dominance in the Gα-QL/DN mutants. Introduction of the QL/DN mutations shifts nucleotide binding specificity from guanine nucleotides to xanthine nucleotides. Because the low concentrations of xanthine nucleotides *in vivo*, essentially nucleotide-free Gα-QL/DN proteins would exist in cells, and these would form stable complexes with cognate receptors and inhibit them by competing

with endogenous wild-type G proteins (Yu *et al.* 2000). Accordingly, it could be expected that all signalling pathways lying on a given receptor became inhibited by any Gα-QL/DN variant interacting with it. Our results demonstrate that this is not the case for the TRH-R. The presence of a heterogeneous population of binding sites for TRH in GH_3 cells has been previously reported (Gautvik & Lystad, 1981) and two TRH-R isoforms derived from the same gene by differential splicing mechanisms have been shown to be expressed in GH_3

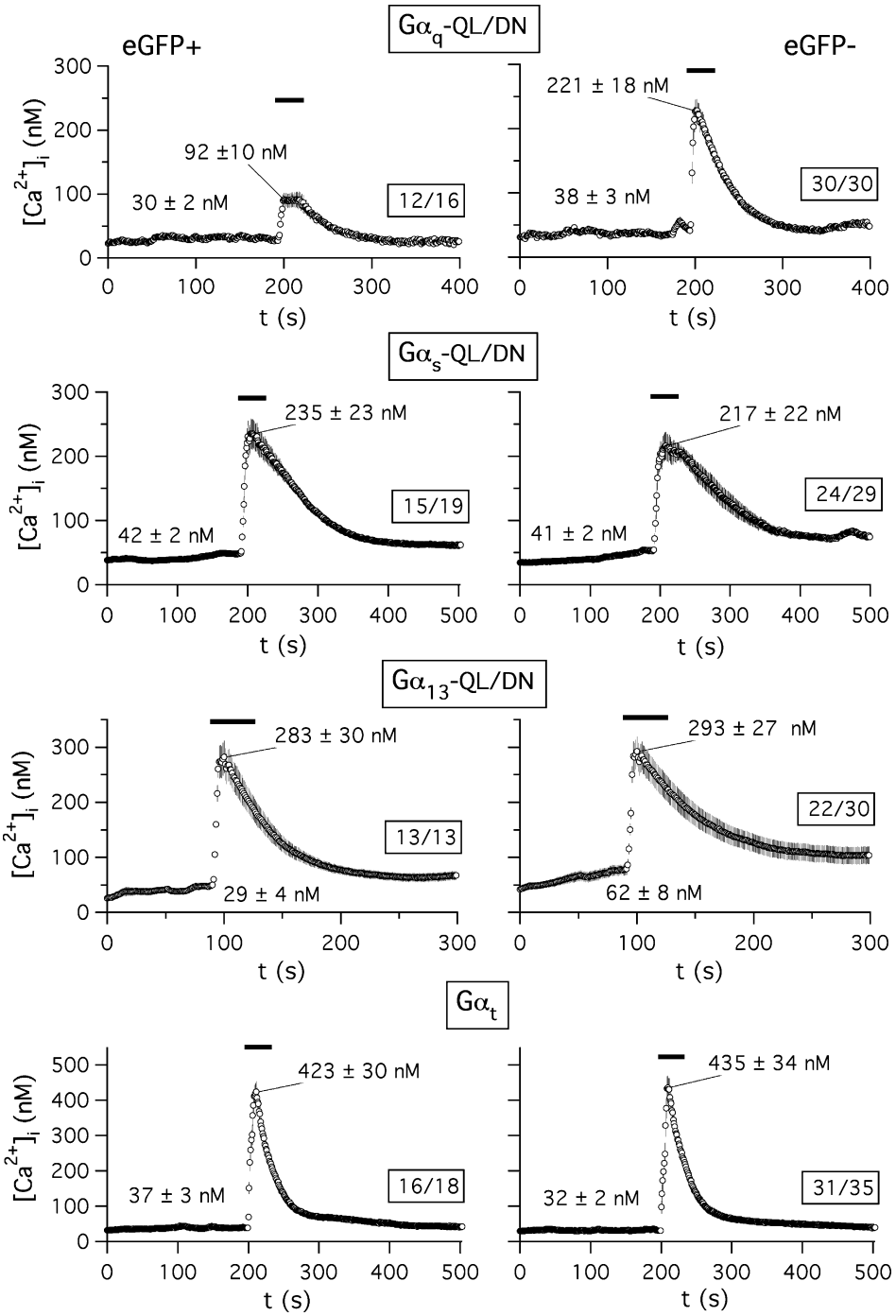

Figure 7. Effect of dominant-negative Gα subunits and Gα_t expression on Ca^{2+} liberation from HEK-H36/T1 cell intracellular stores in response to TRH

Protocols and data evaluation were performed as described in Fig. 2. Only data from the cell subpopulations showing a visually detectable peak Ca^{2+} increase are plotted. In all cases the number of averaged cells respect to the total number of cells present in the field is boxed. Analogous results were obtained in two additional experiments.

cells (de la Peña *et al.* 1992). However, no significant differences in binding or signalling properties of these receptors seem to exist (de la Peña *et al.* 1992; Lee *et al.* 1995; Gershengorn & Osman, 1996). Furthermore, the presence of two different molecular species of TRH-R could not explain the dominant-negative specificity found in HEK-H36/T1 cells in which only an isoform of the receptor is expressed. Clearly, further work will be necessary to understand the reason(s) for the observed specificity of the dominant-negative effects.

Regardless of the exact mechanism by which the negative dominance takes place, the demonstration of the functionality and specificity of the Gα-QL/DN variants allowed us to explore the TRH-R coupling to defined G proteins for transducing the inhibitory signal to ERG channels. Our results suggest that Gα_s plays a crucial role transducing the TRH signal to native r-ERG channels in GH_3 cells, since dominant-negative Gα_s causes the greatest reduction of the hormonal effect as well as the smallest data dispersion in individual cells. These data are consistent with previous results showing that the TRH-induced r-ERG inhibition is enhanced by short-term treatment with cholera toxin (an agent able to specifically modify Gα_s functionality) and nearly abolished when the

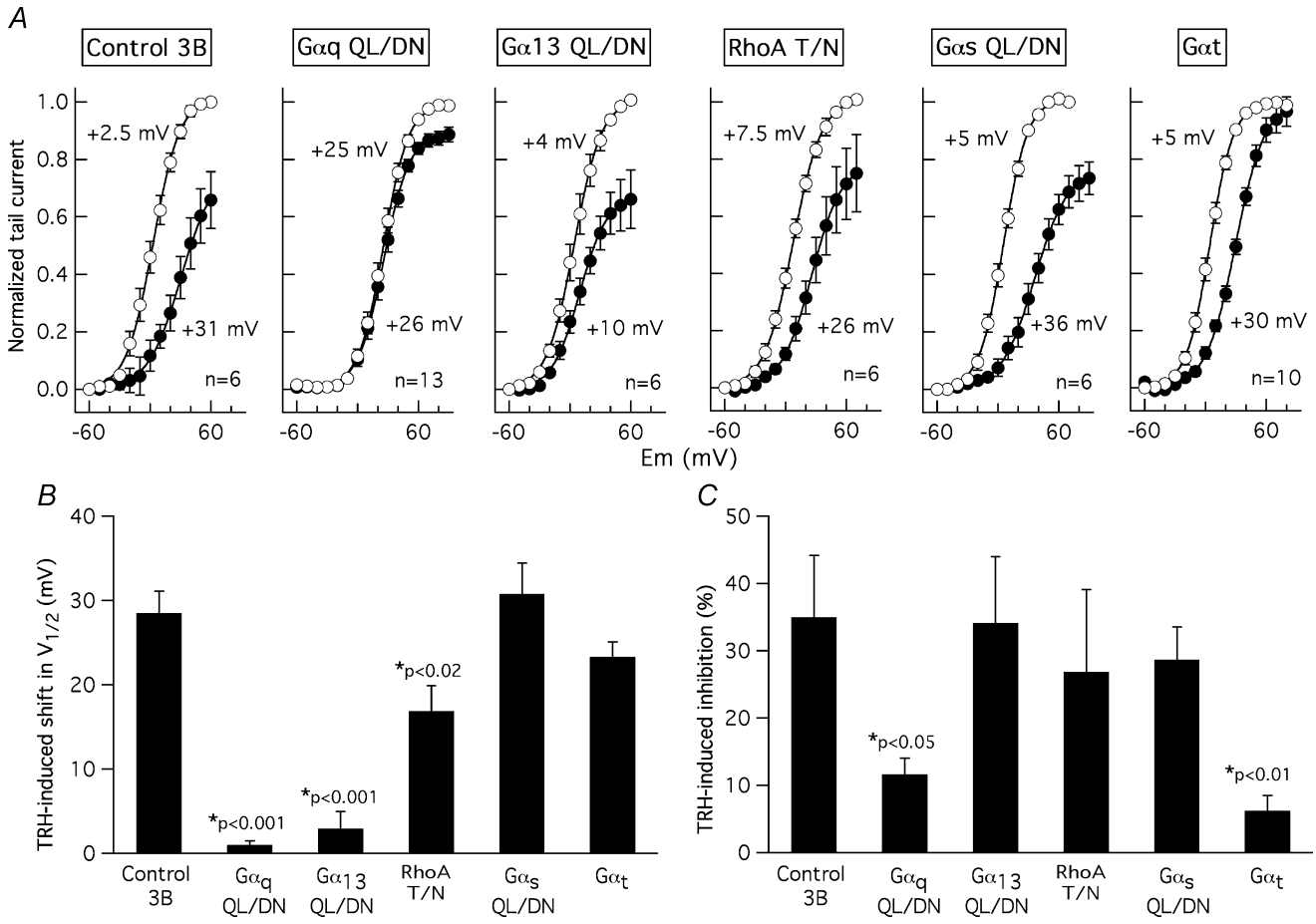

Figure 8. Effect of dominant-negative Gα subunits and Gα_t on TRH-induced modifications of HERG *I–V* curves in HEK-H36/T1 cells

A, effect of Gα subunit expression on HERG activation voltage dependence. Voltage dependence of activation was studied in the absence (open symbols) or the presence (filled symbols) of 1 μM TRH by varying the magnitude of a 1 s depolarizing pulse as detailed in the legend of Fig. 5*A*. Data normalized to maximum of tail current magnitude without TRH are shown. $V_{1/2}$ values obtained from the Boltzmann curves that best fitted the averaged data (continuous lines) and the number of recorded cells are indicated in the graphs. *B*, comparison of TRH-induced shifts on activation voltage dependence in cells expressing different Gα subunits. Data from the same cells used to generate the averaged *I–V* curves shown in panel *A* were used. Values of TRH-induced shifts from the different individual cells were averaged and are shown in the histogram. *C*, effect of Gα subunit expression on TRH-induced inhibition of HERG currents at positive voltages. Data from the same cells used to generate the averaged *I–V* curves shown in panel *A* were used. Values of TRH-induced reductions in maximal currents from the different individual cells were averaged and are shown in the histogram. Statistically significant variations *versus* controls in Student's *t* or Mann-Whitney tests are indicated in *B* and *C*.

treatment with the toxin is prolonged (Barros *et al.* 1993, 1994; Bauer *et al.* 1994). They will be also coherent with the reported inhibition of TRH-induced PLC stimulation in *Xenopus* oocytes using nucleotides antisense to $G\alpha_s$ (de la Peña *et al.* 1995; but see Gershengorn & Osman, 1996). The reasons why coupling of TRH-R to G_s in GH_3 cells only modestly stimulates adenylyl cyclase (Paulssen *et al.* 1992; Gershengorn & Osman, 1996) and why prolonged stimulation with TRH down-regulates $G_{q/11}$ but has no effect on the $G\alpha_s$ protein levels (Kim *et al.* 1994) remain to be established. As suggested previously (Barros *et al.* 1993, 1994; Bauer *et al.* 1994), it is possible that a G_s-like protein that is not G_s itself, but sensitive to cholera toxin and blocked by $G\alpha_s$-QL/DN expression, is involved in GH_3 cell r-ERG inhibition by TRH.

Using the dominant-negative approach we also studied the possible implication of $G\alpha_{13}$ and RhoA, two entities recently proposed as mediators of r-ERG modulation by TRH (Storey *et al.* 2002). In this case, expression of dominant-negative $G\alpha_{13}$-QL/DN significantly reduced the TRH-induced inhibition, although a slightly smaller effect was observed than that with $G\alpha_s$-QL/DN and only in around 50% of the recorded cells was the hormonal effect clearly antagonized. It is unlikely that this situation is caused by an unspecific inhibition of G_s by dominant-negative $G\alpha_{13}$ because smaller TRH-induced inhibitions and wider dispersion of the data were also observed with dominant-negative RhoA, a component located downstream of G_{13} in many cellular systems and (supposedly) not directly related to G_s. On the other hand, it seems difficult to conceive a transduction mechanism involving $G\alpha_s$, $G\alpha_{13}$ and RhoA (but not $G\alpha_q$) either simultaneously or indistinctly. Our data following the overexpression of $G\alpha_t$, an agent known to sequester free G-protein $\beta\gamma$ dimers (Crespo *et al.* 1994; Faure *et al.* 1994; Palomero *et al.* 1998), offer a possible explanation of this apparent paradox. Thus, prominent reductions of the TRH-induced r-ERG inhibition equivalent to those obtained with dominant-negative $G\alpha_s$ are observed in $G\alpha_t$-transfected GH_3 cells. The specificity of the $G\alpha_t$ effect was demonstrated by its failure to modify the Ca^{2+} response in the same cells. It is tempting to speculate that a specific set of free $\beta\gamma$ subunits released from G_s heterotrimers (or a similar combination present in G_{13} but not in G_q) may be responsible for the TRH-induced inhibition of endogenous r-ERG currents in GH_3 cells. Interestingly, both G_α and $G_{\beta\gamma}$ subunits have been implicated in activation of Rho (Niu *et al.* 2003). Furthermore, GH_3 cells constitute perhaps the best characterized example in which specific hormone receptors have been shown to use G protein heterotrimers of different $\alpha\beta\gamma$ subunit composition to modulate an ionic channel (reviewed in Robishaw & Berlot, 2004).

Comparison of TRH and dominant-negative effects in native GH_3 cells and a heterologous expression system such as the HEK-H36/T1 cells reveals some quantitative and qualitative differences. These include (i) considerably smaller TRH-induced current inhibitions in HEK-H36/T1 cells, (ii) a clear inability of dominant-negative $G\alpha_s$ to alter TRH-induced modifications of both activation voltage dependence and HERG current magnitude in HEK-H36/T1 cells, (iii) a significant reduction of the *I–V* curve shifts induced by TRH in HEK-H36/T1 cells upon expression of $G\alpha_{13}$-QL/DN and RhoA-T/N without any concomitant alteration of current inhibition, and (iv) the maintenance of a TRH-induced positive shift of the *I–V* curves in $G\alpha_t$-transfected HEK-H36/T1 cells in which the presence of the $\beta\gamma$ scavenger abolishes the HERG current inhibition induced by the hormone. Use of perforated-patch conditions excludes uncontrolled alterations of the intracellular environment as a cause for these differences. Instead, our results point to differences in the cellular background and/or the molecular identity of the channel protein as determinant of them. The parallel effects of TRH on ERG channels either endogenous or overexpressed in GH_3/B_6 cells (Schledermann *et al.* 2001) suggest that the cellular background may influence the transduction mechanism(s) involved in hormonal regulation of the channels. This is further supported by recent results showing that $G_{q/11}$, but not $G_{i/o}$ or G_{13}, mediates hormonal inhibition of ERG currents in tsA-201 cells coexpressing rat ERG1 channels and another $G_{q/11}$-coupled receptor, the M1 muscarinic receptor (Hirdes *et al.* 2004). Some differences between the signal cascade mediating the TRH-induced modulation of HERG in *Xenopus* oocytes and the physiological pathway modulating the native ERG channels in GH_3 cells have been also reported (Barros *et al.* 1998). It is important to highlight that the dominant-negative effects reported here may vary also as a function of the kinetic parameter being considered. Thus whereas only an attenuation of the TRH-induced *I–V* shifts is observed in HEK-H36/T1 cells in which the G_{13} pathway is blocked with dominant-negative G_{13} or RhoA, only the hormone-induced current inhibition but not the *I–V* shift is antagonized in $G\alpha_t$-transfected cells. The possibility that more than one hormone-activated mechanism exists for regulation of different channel properties is reinforced by recent data showing that separate protein segments in the amino terminus and/or different structural rearrangements of the channel molecule are necessary for the TRH-induced modifications of HERG activation and deactivation gating in *Xenopus* oocytes (Gómez-Varela *et al.* 2003*a*).

In summary, the results presented in this report lead us to propose that free $\beta\gamma$ subunits released from G_s (and perhaps shared by G_{13}) heterotrimers are responsible for

TRH-induced inhibition of the endogenous r-ERG current in GH_3 cells, in which reductions of current magnitude constitute the major component of the hormonal response. Differences in the subunit composition of the $\beta\gamma$ dimers associated with G_q could explain the inability of G_q heterotrimers to serve a similar function in these cells. Variations in the cellular background upon heterologous expression of the channels may influence the transduction mechanism(s) involved in hormonal regulation of ERG, but also the kinetic characteristics modified in response to an agonist. Thus, as suggested by the similarities in the effects of $G\alpha_q$-QL/DN and $G\alpha_t$, $\beta\gamma$ dimers released from a G protein different from G_s (probably G_q) are probably involved in the relatively small current inhibition detected in HEK-H36/T1 cells. However, it is a $G\alpha_{13}$- and RhoA-dependent pathway what seems to determinate the prominent alterations in HERG activation voltage dependence triggered by TRH in these cells heterologously expressing HERG channels and TRH-Rs.

References

Akita Y, Ohno S, Yajima Y, Konno Y, Saido TC, Mizuno K *et al.* (1994). Overproduction of a Ca^{2+}-independent protein kinase C isozyme, nPKCε, increases the secretion of prolactin from thyrotropin-releasing hormone-stimulated rat pituitary GH4C1 cells. *J Biol Chem* **269**, 4653–4660.

Barros F, del Camino D, Pardo LA, Palomero T, Giráldez T & de la Peña P (1997). Demonstration of an inwardly rectifying K^+ current component modulated by thyrotropin-releasing hormone and caffeine in GH_3 rat anterior pituitary cells. *Pflugers Arch* **435**, 119–129.

Barros F, Delgado LM, del Camino D & de la Peña P (1992). Characteristics and modulation by thyrotropin-releasing hormone of an inwardly rectifying K^+ current in patch-perforated GH_3 anterior pituitary cells. *Pflugers Arch* **422**, 31–39.

Barros F, Delgado LM, Maciá C & de la Peña P (1991). Effects of hypothalamic peptides on electrical activity and membrane currents of 'patch perforated' clamped GH_3 anterior pituitary cells. *FEBS Lett* **279**, 33–37.

Barros F, Gómez-Varela D, Viloria CG, Palomero T, Giráldez T & de la Peña P (1998). Modulation of human erg K^+ channel gating by activation of a G protein-coupled receptor and protein kinase C. *J Physiol* **511**, 333–346.

Barros F, Mieskes G, del Camino D & de la Peña P (1993). Protein phosphatase 2A reverses inhibition of inward rectifying K^+ currents by thyrotropin-releasing hormone in GH_3 pituitary cells. *FEBS Lett* **336**, 433–439.

Barros F, Villalobos C, García-Sancho J, del Camino D & de la Peña P (1994). The role of the inwardly rectifying K^+ current in resting potential and thyrotropin-releasing hormone-induced changes in cell excitability of GH_3 rat anterior pituitary cells. *Pflugers Arch* **426**, 221–230.

Bauer CK (1998). The erg inwardly rectifying K^+ current and its modulation by thyrotropin-releasing hormone in giant clonal rat anterior pituitary cells. *J Physiol* **510**, 63–70.

Bauer CK, Davison I, Kubasov I, Schwarz JR & Mason WT (1994). Different G proteins are involved in the biphasic response of clonal rat pituitary cells to thyrotropin-releasing hormone. *Pflugers Arch* **428**, 17–25.

Bauer CK, Engeland B, Wulfsen I, Ludwig J, Pongs O & Schwarz JR (1998). RERG is a molecular correlate of the inward-rectifying K current in clonal rat pituitary cells. *Receptors Channels* **6**, 19–29.

Bauer CK, Meyerhof W & Schwarz JR (1990). An inward-rectifying K^+ current in clonal rat pituitary cells and its modulation by thyrotropin-releasing hormone. *J Physiol* **429**, 169–189.

Bauer CK, Schäfer R, Schiemann D, Reid G, Hanganu I & Schwarz JR (1999). A functional role of the erg-like inward-rectifying K^+ current in prolactin secretion from rat lactotrophs. *Mol Cell Endocrinol* **148**, 37–45.

Bian J, Cui J & McDonald TV (2001). HERG K^+ channel activity is regulated by changes in phosphatidyl inositol 4,5-bisphosphate. *Circ Res* **89**, 1168–1176.

Chang F-H & Bourne HR (1989). Cholera toxin induces cAMP-independent degredation of Gs. *J Biol Chem* **264**, 5352–5357.

Chiang C-E & Roden DM (2000). The long QT syndromes: genetic basis and clinical implications. *J Am Coll Cardiol* **36**, 1–12.

Crespo P, Xu N, Simonds WF & Gutkind JS (1994). Ras-dependent activation of MAP kinase pathway mediated by G-protein $\beta\gamma$ subunits. *Nature* **369**, 418–420.

de la Peña P, del Camino D, Pardo LA, Dominguez P & Barros F (1995). Gs couples thyrotropin-releasing hormone receptors expressed in Xenopus oocytes to phospholipase C. *J Biol Chem* **270**, 3554–3559.

de la Peña P, Delgado LM, del Camino D & Barros F (1992). Two isoforms of the thyrotropin-releasing hormone receptor generated by alternative splicing have indistinguishable functional properties. *J Biol Chem* **267**, 25703–25708.

Dutt P, Kjoller L, Giel M, Hall A & Toksoz D (2002). Activated Gαq family members induce Rho GTPase activation and Rho-dependent actin filament assembly. *FEBS Lett* **531**, 565–569.

Emmi A, Wenzel HJ, Schwatzkroin PA, Taglialatela M, Castaldo P, Bianchi L *et al.* (2000). Do glia have heart? Expression and functional role for *Ether-a-go-go* currents in hippocampal astrocytes. *J Neurosci* **20**, 3915–3925.

Faure M, Voyno-Yasenetskaya TA & Bourne HR (1994). cAMP and $\beta\gamma$ subunits of heterotrimeric G proteins stimulate the mitogen-activated protein kinase pathway in COS-7 cells. *J Biol Chem* **269**, 7851–7854.

Finlayson K, Witchel HJ, McCulloch J & Sharkey J (2004). Adquired QT interval prolongation and HERG: implications for drug discovery and development. *Eur J Pharmacol* **500**, 129–142.

Gautvik KM & Lystad E (1981). Demonstration of a heterogeneous population of binding sites for thyroliberin in prolaction-producing tumour cells and their possible functional significance. *Eur J Biochem* **116**, 235–242.

Gershengorn MC & Osman R (1996). Molecular and cellular biology of thyrotropin-releasing hormone receptors. *Physiol Rev* **76**, 175–191.

Gómez-Varela D, Barros F, Viloria CG, Giráldez T, Manso DG, Dupuy SG *et al.* (2003*a*). Relevance of the proximal domain in the amino-terminus of HERG channels for regulation by a phospholipase C-coupled hormone receptor. *FEBS Lett* **535**, 125–130.

Gómez-Varela D, Giráldez T, de la Peña P, Dupuy SG, García-Manso D & Barros F (2003*b*). Protein kinase C is necessary for recovery from the thyrotropin-releasing hormone-induced r-ERG current reduction in GH_3 rat anterior pituitary cells. *J Physiol* **547**, 913–929.

Gullo F, Ales E, Rosati B, Lecchi M, Masi A, Guasti L *et al.* (2003). ERG K^+ channel blockade enhances firing and epinephrine secretion in rat chromaffin cells: the missing link to LQT2-related sudden death? *FASEB J* **17**, 330–332.

Hirdes W, Horowitz LF & Hille B (2004). Muscarinic modulation of erg potassium current. *J Physiol* **559**, 67–84.

Keating MT & Sanguinetti MC (2001). Molecular and cellular mechanisms of cardiac arrhythmias. *Cell* **104**, 569–580.

Kiley SC, Parker PJ, Fabbro D & Jaken S (1991). Differential regulation of protein kinase C isozymes by thyrotropin-releasing hormone in GH_4C_1 cells. *J Biol Chem* **266**, 23761–23768.

Kim G-D, Carr IC, Anderson LA, Zabavnik J, Eidne KA & Milligan G (1994). The long isoform of the rat thyrotropin-releasing hormone receptor down-regulates G_q proteins. *J Biol Chem* **269**, 19933–19940.

Lastraioli E, Guasti L, Crociani O, Polvani S, Hofmann G, Witchel H *et al.* (2004). herg1 gene and HERG1 protein are overexpressed in colorectal cancers and regulate cell invasion of tumor cells. *Cancer Res* **64**, 606–611.

Lee TW, Anderson LA, Eidne KA & Milligan G (1995). Comparison of the signalling properties of the long and short isoforms of the rat thyrotropin-releasing hormone receptor following expression in Rat 1 fibroblasts. *Biochem J* **310**, 291–298.

Niu J, Profirovic J, Pan H, Vaiskunaite R & Voyno-Yasenetskaya T (2003). G protein $\beta\gamma$ subunits stimulate p114RhoGEF, a guanine nucleotide exchange factor for RhoA and Rac1. Regulation of cell shape and reactive oxygen species production. *Circ Res* **93**, 848–856.

Palomero T, Barros F, del Camino D, Viloria CG & de la Peña P (1998). A G protein $\beta\gamma$ dimer-mediated pathway contributes to mitogen-activated protein kinase activation by thyrotropin-releasing hormone receptors in transfected COS-7 cells. *Mol Pharmacol* **53**, 613–622.

Paulssen RH, Paulssen EJ, Gautvik KM & Gordeladze JO (1992). The thyroliberin receptor interacts directly with a stimulatory guanine-nucleotide-binding protein in the activation of adenylyl cyclase in GH_3 pituitary tumour cells. Evidence obtained by the use of antisense RNA inhibition and immunoblocking of the stimulatory guanine-nucleotide-binding protein. *Eur J Biochem* **204**, 413–418.

Petrecca K, Atanasiu R, Akhavan A & Shrier A (1999). N-linked glycosilation sites determine HERG channel surface membrane expression. *J Physiol* **515**, 41–48.

Redfern WS, Carlsson L, Davis AS, Lynch WG, MacKenzie I, Palethorpe S *et al.* (2003). Relationships between preclinical cardiac electrophysiology, clinical QT interval prolongation and torsade de pointes for a broad range of drugs: evidence for a provisional safety margin in drug development. *Cardiovasc Res* **58**, 32–45.

Robishaw JD & Berlot CH (2004). Translating G protein subunit diversity into functional specificity. *Curr Op Cell Biol* **16**, 206–209.

Rosati B, Marchetti P, Crociani O, Lecchi M, Lupi R, Arcangeli A *et al.* (2000). Glucose- and arginine-induced insulin secretion by human pancreatic β-cells: the role of HERG K^+ channels in firing and release. *FASEB J* **14**, 2601–2610.

Sacco T, Bruno A, Wanke E & Tempia F (2003). Functional roles of an ERG current isolated in cerebellar Purkinje neurons. *J Neurophysiol* **90**, 1817–1828.

Sah VP, Seasholtz TM, Sagi SA & Brown JH (2000). The role of Rho in G protein-coupled receptor signal transduction. *Annu Rev Pharmacol Toxicol* **40**, 459–489.

Schäfer R, Wulfsen I, Behrens S, Weinsberg F, Bauer CK & Schwarz JR (1999). The erg-like current in rat lactotrophs. *J Physiol* **518**, 401–416.

Schledermann W, Wulfsen I, Schwarz JR & Bauer CK (2001). Modulation of rat erg1, erg2, erg3 and HERG K^+ currents by thyrotropin-releasing hormone in anterior pituitary cells via the native signal cascade. *J Physiol* **532**, 143–163.

Schönherr R, Rosati B, Hehl S, Rao VG, Arcangeli A, Olivotto M & Wanke E (1999). Functional role of the slow activation property of ERG K^+ channels. *Eur J Neurosci* **11**, 753–760.

Seasholtz TM, Majumdar M & Brown JH (1999). Rho as a mediator of G protein-coupled receptor signaling. *Mol Pharmacol* **55**, 949–956.

Storey NM, O'Brian JP & Armstrong DL (2002). Rac and Rho mediate opposing hormonal regulation of the ether-a-go-go-related potassium channel. *Curr Biol* **12**, 27–33.

Thomas D, Kiehn J, Katus HA & Karle CA (2004). Adrenergic regulation of the rapid component of the cardiac delayed rectifier potassium current, I_{Kr}, and the underlying hERG ion channel. *Basic Res Cardiol* **99**, 279–287.

Viloria C, Barros F, Giráldez T, Gómez-Varela D & de la Peña P (2000). Differential effects of amino-terminal distal and proximal domains in the regulation of human *erg* K^+ channel gating. *Biophys J* **79**, 231–246.

Vogt S, Grosse R, Schultz G & Offermanns S (2003). Receptor-dependent RhoA activation in G_{12}/G_{13}-deficient cells. Genetic evidence for an involvement of G_q/G_{11}. *J Biol Chem* **278**, 28743–28749.

Weinsberg F, Bauer CK & Schwarz JR (1997). The class III antiarrhythmic agent E-4031 selectively blocks the inactivating inward-rectifying potassium current in rat anterior pituitary tumor cells (GH_3/B_6 cells). *Pflugers Arch* **434**, 1–10.

Yajima Y, Akita Y & Saito T (1988). Effects of cholera toxin on the coupling of thyrotropin-releasing hormone to a guanine nucleotide-binding protein in cultured GH_3 cells. *Mol Pharmacol* **33**, 592–597.

Yu B, Gu L & Simon MI (2000). Inhibition of subsets of G protein-coupled receptors by empty mutants of G protein α subunits in G_o, G_{11}, and G_{16}. *J Biol Chem* **275**, 71–76.

Zhou W, Cayabyab FS, Pennefather PS, Schlichter LC & De Coursey TE (1998*a*). HERG-like K^+ channels in microglia. *J General Physiol* **111**, 781–794.

Zhou Z, Gong QYeB, Fan Z, Makielski JC, Robertson GA & January CT (1998*b*). Properties of HERG channels stably expressed in HEK 293 cells studied at physiological temperature. *Biophys J* **74**, 230–241.

Acknowledgements

We thank Noelia S. Durán for technical assistance. We also thank Drs Maria Sierra, Miguel A. Comendador and Pelayo Casares for help with statistical analysis. This work was supported by grants PM99-0152 and SAF2003-00329 from DGICYT and Ministerio de Ciencia y Tecnología of Spain. Finance support from Dirección Gral. de Universidades e Investigación of Asturias for acquisition of the image equipment (ref. EQPT02-36) is also acknowledged. P.M. holds a predoctoral fellowship from FICYT of Asturias (ref. BP03-108). D.G., C.A.R. and D.G.V. are predoctoral fellows from the Spanish Ministerio de Ciencia y Tecnología (refs AP2000-4363, BES-2004-3872 and FP2000-5736).